Current Biology

The conserved endocannabinoid anandamide modulates olfactory sensitivity to induce hedonic feeding in C. elegans

--Manuscript Draft--

Manuscript Number:	CURRENT-BIOLOGY-D-23-00175R1
Full Title:	The conserved endocannabinoid anandamide modulates olfactory sensitivity to induce hedonic feeding in C. elegans
Article Type:	Research Article
Corresponding Author:	Shawn Lockery University of Oregon Eugene, Oregon UNITED STATES
First Author:	Anastasia Levichev
Order of Authors:	Anastasia Levichev
	Serge Faumont
	Rachel Z. Berner
	Zhifeng Purcell
	Amanda M. White
	Kathy Chicas-Cruz
	Shawn Lockery
Abstract:	The ability of cannabis to increase consumption of food has been known for centuries. In addition to producing hyperphagia, cannabinoids can amplify existing preferences for calorically dense, palatable food sources, a phenomenon called hedonic amplification of feeding. These effects result from the action of plant-derived cannabinoids that mimic endogenous ligands called endocannabinoids. The high degree of conservation of cannabinoid signaling at the molecular level across the animal kingdom suggests hedonic feeding may also be widely conserved. Here we show that exposure of C. elegans to anandamide, an endocannabinoid common to nematodes and mammals, shifts both appetitive and consummatory responses toward nutritionally superior food, an effect analogous to hedonic feeding. We find that anandamide's effect on feeding requires the C. elegans cannabinoid receptor NPR-19 but can also be mediated by the human CB1 cannabinoid receptor, indicating functional conservation between the nematode and mammalian endocannabinoid systems for regulation of food preferences. Furthermore, Anandamide has reciprocal effects on appetitive and consummatory responses to food, increasing and decreasing responses to inferior and superior food respectively. Anandamide's behavioral effects require the AWC chemosensory neurons, and anandamide renders these neurons more sensitive to superior food and less sensitive to inferior food, mirroring the reciprocal effects seen at the behavioral level. Our findings reveal a surprising degree of functional conservation in the effects of endocannabinoids on hedonic feeding across species and establish a new system to investigate the cellular and molecular basis of endocannabinoid system function in the regulation of food choice.
Additional Information:	
Question	**Response**
Standardized datasets A list of datatypes considered standardized under Cell Press policy is available here. Does this manuscript report new standardized datasets?	No
Original Code	No

Does this manuscript report original code?	

My colleagues and I are pleased to resubmit for your consideration the manuscript *The conserved endocannabinoid anandamide modulates olfactory sensitivity to induce hedonic feeding in* C. elegans.

In separate studies over the last 10 years, we have been investigating food choice in *C. elegans* as a model for value-based decision making. The present study has an interesting origin. In almost literally a "Friday afternoon experiment," which occurred shortly after cannabis was legalized in Oregon, we decided to see if soaking worms in endocannabinoid alters existing food preferences. It does. In particular, it makes worms more hungry for their favored foods and less hungry for non-favored foods. Thus, the effects of endocannabinoid in nematodes parallels the effects of marijuana on human appetites. The surprising nature of these findings, together with growing public interest in cannabis products, suggests that our research will likely be of interest to the broad readership of Current Biology.

Thank you in advance for your consideration.

We were very pleased to hear that the referees and editor found our paper, "The conserved endocannabinoid anandamide modulates olfactory sensitivity to induce hedonic feeding in *C. elegans*" of sufficient interest to publish in Current Biology, pending our response to Referee 1. As this Response Letter indicates, we believe we have addressed all major and minor concerns of Referee 1. The other referees reported no concerns.

Acceptance of this paper on or before April 1, 2023 would allow us to report its change of status to NIH in time for review of a major grant. We would be sincerely grateful if this deadline could be met.

We intend to submit a Figure360 video. However, relative to the above deadline, we ask permission to prepare and submit this material while the paper is being readied for publication. Please let us know if this request is acceptable.

Major

1. It seems that this phenotype requires very high concentrations of AEA to observe its effects (100 µM or 300 µM) and the authors state "The incubation time and relatively high concentration reflects the low permeability of the C. elegans cuticle to exogenous molecules". Is there a dose dependent effect on these behaviours? Is there no phenotype at all at lower concentrations? I could not find anything related to this in this study or others (e.g., Oakes et al 2017). The authors should include some assays across different AEA concentrations or reference where this can be found to explain the 100 µM or 300 µM concentrations.

It is standard practice in *C. elegans* pharmacology to expose intact worms to high doses of test compounds (Davies *et al.*, 2003; Rand and Johnson, 1995; Vidal-Gadea *et al.*, 2012). As mentioned in the text, this is done to overcome the permeation barrier presented by the worm's protective cuticle. We based our AEA dosage on Oakes et al., 2017, Fig. 4E (below), which shows how inhibition of pharyngeal pumping varies as a function the concentration of AEA and 2-AG, a related endocannabinoid.

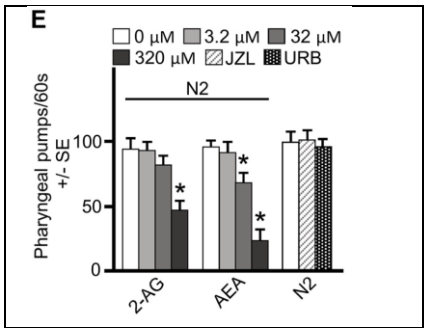

E, Concentration-dependent 2-arachidonoylglycerol (2-AG) and anandamide (AEA) inhibition of pharyngeal pumping (M. Oakes *et al.*, 2017).

Furthermore, in pilot pumping-rate and T-maze assays, we did use lower AEA doses (100 μM and 50 μM, respectively). However, these experiments revealed small, variable effects, so we settled on the somewhat higher doses used in this study (300 μM and 100 μM, respectively). These doses are nevertheless within the effective range demonstrated by Oakes et al. They are also within the range required to elicit all known endocannabinoid phenotypes in *C. elegans* including inhibition of dauer formation, axon regeneration, nociception, and locomotion (Estrada-Valencia *et al.*, 2021). In the text, we now refer to the Oakes et al. study, and explain how we arrived and the AEA concentrations used (lines 586-593).

Finally, one of the main concerns with high doses of a drug is the emergence of off-target effects. However, the complete absence of AEA effects on appetitive behavior in two independent alleles of *npr-19* mutants (Fig. 4A) makes this possibility unlikely.

Minor

1. Intro paragraph line 70 to 78 should state these studies were performed in rats.

Done (line 76).

2. Line 102 "line" should be replaced with "lineage".

Done (line 102).

3. I found it a bit odd that OP50 (Fig S1) is not part of fig 1B even if it has been reported previously. It is after all the classical food source and it would be nice to have it as a reference alongside the other bacteria in fig 1B.

OP50 was not included in Fig. 1B (now Fig. 1C) because its quality as a food source was not measured in the study we used to arrange pumping rate data along the continuum from superior to inferior (Avery and Shtonda, 2003). In response to the reviewer's suggestion, we have moved the OP50 data to Fig. 1, panel A2. For consistency with the inclusion of OP50 data, the EPG traces used to illustrate the methodology were changed in Fig. 1, panel A1, which originally showed feeding DA1877 and DA1885 bacteria, were replaced by traces showing feeding in OP50 bacteria.

4.1. Line 216: Could the authors clarify the function of *ceh-36* further for a none nematode researcher e.g. "the C. elegans Homeodomain Transcription Factor gene *ceh-36* involved in ….".

Done (line 218-219).

4.2. Additionally, is ASE function not also impaired in the ceh-36 mutant?

We are not aware of any recordings from ASE neurons in response to chemosensory inputs in *ceh-36* mutants. Genetic evidence indicates that whereas in AWC *ceh-36* is required for basal neuronal functionality, in ASE it is required only for left-right differences in ASE-

neuron taste transduction (Lanjuin *et al.*, 2003). Therefore, functional impairments, if any, are likely to be minor. Furthermore, in our study (and many others) food choice is driven mainly by distal odors, not tastes (Fig. 3A,B). Although ASE does respond to odors, these are indirect responses inherited from AWC via peptidergic signaling, which bypasses ASE transduction mechanisms (Leinwand *et al.*, 2015). Therefore, any ASE impairments are almost certainly irrelevant to the interpretation of *ceh-36* mutants in our study. This information has been added to the manuscript (lines 220-223).

5. Are there other cannabinoid-like receptors or is *npr-19* the only C. elegans cannabinoid-like receptor? This should be stated somewhere in the manuscript.

NPR-19 is the only receptor that has been shown to respond to AEA in a heterologous expression system (M. D. Oakes *et al.*, 2017). An additional receptor, OCTR-1, has been shown to respond to high concentrations of 2-AG in a heterologous expression system but was not tested for a response to AEA (M. D. Oakes *et al.*, 2017). Additionally, genetic evidence suggests that the G-protein coupled receptor *npr-32*, the TRPV-like channel *osm-9*, and TRPN-like channel *trp-4* may also act as receptors. This information has been added to the manuscript (lines 104-106).

6. Line 218: the "x" in this sentence is odd to read.

Changed “strain × AEA interaction” to “strain by AEA interaction” here and throughout.

7. Line 222: Why are "decreases" and "attraction" italicized?

Removed italicization.

8. In the text running order, table 6 is referenced before table 5 therefore they should be inverted.

Fixed.

9. Line 385-388: This paragraph begins by talking about a model. It might be nice to have an additional figure panel illustrating this.

We have added this figure to the Discussion (Fig. 6).

10. Table 1: some text is missing "Cell body position and …."

Fixed.

11. Materials and methods section
a. Line 567: What is the background solution? It is unclear if this is M9 or A0?

We clarified which buffer was used in the different types of experiments (lines 583-587).

b. Line 619: there is some text missing between the and and bracket "and (25"

Now reads “Critically, the percentage of non-responders did not vary between AEA-treated and non-treated animals (25.46% vs 22.49% respectively; $\chi^2(1,759) = 0.699$, $p = 0.4031$).”

c. Line 629: The figure number is missing "(Fig.)"

Fixed.

References

Avery, L. and Shtonda, B. B. (2003) ‘Food transport in the C. elegans pharynx’, *Journal of Experimental Biology*. doi: 10.1242/jeb.00433.

Davies, A. G. *et al.* (2003) ‘A Central Role of the BK Potassium Channel in Behavioral Responses to Ethanol in C. elegans’, *Cell*. Cell Press, 115(6), pp. 655–666. doi: 10.1016/S0092-8674(03)00979-6.

Estrada-Valencia, R. *et al.* (2021) ‘The Endocannabinoid System in Caenorhabditis elegans’, (August 2021), pp. 1–31. doi: 10.1007/112_2021_64.

Lanjuin, A. *et al.* (2003) ‘Otx / otd Homeobox Genes Specify Distinct Sensory Neuron Identities in C . elegans’, *Developmental Cell*, 5, pp. 621–633.

Leinwand, S. G. *et al.* (2015) ‘Circuit mechanisms encoding odors and driving aging-associated behavioral declines in Caenorhabditis elegans’, *eLife*, 4(September 2015), pp. 1–26. doi: 10.7554/eLife.10181.

Oakes, M. *et al.* (2017) ‘Cannabinoids activate monoaminergic signaling to modulate key C. elegans behaviors’, *Journal of Neuroscience*. Society for Neuroscience, 37(11), pp. 2859–2869. doi: 10.1523/JNEUROSCI.3151-16.2017.

Oakes, M. D. *et al.* (2017) ‘Cannabinoids Activate Monoaminergic Signaling to Modulate KeyC. elegansBehaviors.’, *The Journal of neuroscience : the official journal of the Society for Neuroscience*. Society for Neuroscience, 37(11), pp. 2859–2869. doi: 10.1523/JNEUROSCI.3151-16.2017.

Rand, J. B., & Johnson, C. D. (1995). Genetic pharmacology: interactions between drugs and gene products in Caenorhabditis elegans. *Methods in cell biology*, *48*, 187–204. https://doi.org/10.1016/s0091-679x(08)61388-6

Vidal-Gadea, A. G., Davis, S., Becker, L., & Pierce-Shimomura, J. T. (2012). Coordination of behavioral hierarchies during environmental transitions in *Caenorhabditis elegans*. *Worm*, *1*(1), 5–11. https://doi.org/10.4161/worm.19148

CELL PRESS DECLARATION OF INTERESTS POLICY

Transparency is essential for a reader's trust in the scientific process and for the credibility of published articles. At Cell Press, we feel that disclosure of competing interests is a critical aspect of transparency. Therefore, we require a "declaration of interests" section in which all authors disclose any financial or other interests related to the submitted work that (1) could affect or have the perception of affecting the author's objectivity or (2) could influence or have the perception of influencing the content of the article.

What types of articles does this apply to?

We require that you disclose competing interests for all submitted content by completing and submitting the "declaration of interests" form below. We also require that you include a "declaration of interests" section in the text of all articles even if there are no interests to declare. Some article types may be exempt; please consult your paper's handling editor with any questions.

What should I disclose?

We require that you and all authors disclose any personal financial interests (examples include stocks or shares in companies with interests related to the submitted work or consulting fees from companies that could have interests related to the work), professional affiliations, advisory positions, board memberships (including membership on a journal's advisory board when publishing in that journal), or patent holdings that are related to the subject matter of the contribution. As a guideline, you need to declare an interest for (1) any affiliation associated with a payment or financial benefit exceeding $10,000 p.a. or 5% ownership of a company or (2) research funding by a company with related interests. You do not need to disclose diversified mutual funds, 401ks, or investment trusts.

Authors should also disclose relevant financial interests of immediate family members. Cell Press uses the Public Health Service definition of "immediate family member," which includes spouse and dependent children.

Where do I declare competing interests?

Competing interests should be disclosed on the "declaration of interests" form as well as in a "declaration of interests" section of the manuscript. This section should include financial or other competing interests as well as affiliations that are not included in the author list. Examples of "declaration of interests" language include:

> "AUTHOR is an employee and shareholder of COMPANY."
> "AUTHOR is a founder of COMPANY and a member of its scientific advisory board."

NOTE: Primary affiliations should be included on the title page of the manuscript with the author list and do not need to be included in the "declaration of interests" section. Funding sources should be included in the "acknowledgments" section and also do not need to be included in the "declaration of interests" section. (A small number of front-matter article types do not include an "acknowledgments" section. For these articles, reporting of funding sources is not required.)

What if there are no competing interests to declare?

If you have no competing interests to declare, please note that in the "declaration of interests" section with the following wording:

> "The authors declare no competing interests."

CELL PRESS DECLARATION OF INTERESTS FORM

If submitting materials via Editorial Manager, please complete this form and upload with your final submission. Otherwise, please email as an attachment to the editor handling your manuscript.

Please complete each section of the form and insert any necessary "declaration of interests" statement in the text box at the end of the form. A matching statement should be included in a "declaration of interests" section in the manuscript.

Institutional affiliations

We require that you list the current institutional affiliations of all authors, including academic, corporate, and industrial, on the title page of the manuscript. ***Please select one of the following:***

- ○ All affiliations are listed on the title page of the manuscript.
- ◉ I or other authors have additional affiliations that we have noted in the "declaration of interests" section of the manuscript and on this form below.

Funding sources

We require that you disclose all funding sources for the research described in this work. ***Please confirm the following:***

- ◉ All funding sources for this study are listed in the "acknowledgments" section of the manuscript.*

*A small number of front-matter article types do not include an "acknowledgments" section. For these, reporting funding sources is not required.

Competing financial interests

We require that authors disclose any financial interests and any such interests of immediate family members, including financial holdings, professional affiliations, advisory positions, board memberships, receipt of consulting fees, etc., that:

(1) could affect or have the perception of affecting the author's objectivity, *or*
(2) could influence or have the perception of influencing the content of the article.

Please select one of the following:

- ○ We, the authors and our immediate family members, have no financial interests to declare.
- ◉ We, the authors, have noted any financial interests in the "declaration of interests" section of the manuscript and on this form below, and we have noted interests of our immediate family members.

Advisory/management and consulting positions

We require that authors disclose any position, be it a member of a board or advisory committee or a paid consultant, that they have been involved with that is related to this study. We also require that members of our journal advisory boards disclose their position when publishing in that journal. ***Please select one of the following:***

- (●) We, the authors and our immediate family members, have no positions to declare and are not members of the journal's advisory board.
- ( ) The authors and/or their immediate family members have management/advisory or consulting relationships noted in the "declaration of interests" section of the manuscript and on this form below.

Patents

We require that you disclose any patents related to this work by any of the authors or their institutions. ***Please select one of the following:***

- ( ) We, the authors and our immediate family members, have no related patents to declare.
- (●) We, the authors, have a patent related to this work, which is noted in the "declaration of interests" section of the manuscript and on this form below, and we have noted the patents of immediate family members.

Please insert any "declaration of interests" statements in this space. This exact text should also be included in the "declaration of interests" section of the manuscript. If no authors have a competing interest, please insert the text, "The authors declare no competing interests."

Shawn R. Lockery is co-founder and Chief Technology Officer of InVivo Biosystems, Inc., which manufactures instrumentation for electrophysiological recording of pumping rate in nematodes, and has a patent on the ScreenChip system. The other authors have no competing interests.

On behalf of all authors, I declare that I have disclosed all competing interests related to this work. If any exist, they have been included in the "declaration of interests" section of the manuscript.

Name: Shawn R. Lockery

Manuscript number (if available):

The conserved endocannabinoid anandamide modulates olfactory sensitivity to induce hedonic feeding in *C. elegans*

Anastasia Levichev[1], Serge Faumont[1], Rachel Z. Berner[1], Zhifeng Purcell[1], Amanda M. White[1], Kathy Chicas-Cruz[1], Shawn R. Lockery[1]*

[1] University of Oregon, Institute of Neuroscience, 1245 University of Oregon, Eugene, Oregon, 97403, USA

*Lead contact: Shawn@uoregon.edu

Summary

The ability of cannabis to increase food consumption has been known for centuries. In addition to producing hyperphagia, cannabinoids can amplify existing preferences for calorically dense, palatable food sources, a phenomenon called hedonic amplification of feeding. These effects result from the action of plant-derived cannabinoids that mimic endogenous ligands called endocannabinoids. The high degree of conservation of cannabinoid signaling at the molecular level across the animal kingdom suggests hedonic feeding may also be widely conserved. Here we show that exposure of *C. elegans* to anandamide, an endocannabinoid common to nematodes and mammals, shifts both appetitive and consummatory responses toward nutritionally superior food, an effect analogous to hedonic feeding. We find that anandamide's effect on feeding requires the *C. elegans* cannabinoid receptor NPR-19 but can also be mediated by the human CB1 cannabinoid receptor, indicating functional conservation between the nematode and mammalian endocannabinoid systems for regulation of food preferences. Furthermore, anandamide has reciprocal effects on appetitive and consummatory responses to food, increasing and decreasing

responses to inferior and superior food respectively. Anandamide's behavioral effects require the AWC chemosensory neurons, and anandamide renders these neurons more sensitive to superior food and less sensitive to inferior food, mirroring the reciprocal effects seen at the behavioral level. Our findings reveal a surprising degree of functional conservation in the effects of endocannabinoids on hedonic feeding across species and establish a new system to investigate the cellular and molecular basis of endocannabinoid system function in the regulation of food choice.

Introduction

It has been known for centuries that smoking or ingesting preparations of the plant *Cannabis sativa* stimulates appetite.[1,2] Users report persistent hunger while intoxicated, even if previously satiated. This feeling of hunger is often accompanied by a specific desire for foods that are sweet or high in fat content, a phenomenon colloquially known as "the munchies."[3–8] The effects of cannabinoids on appetite result mainly from Δ^9-tetrahydrobannabinol (THC), a plant-derived cannabinoid. THC acts at cannabinoid receptors in the brain, mimicking endogenous ligands called endocannabinoids, which include anandamide (N-arachidonoylethanolamine, AEA) and 2-arachidonoylglycerol (2-AG). AEA and 2-AG are the best studied signaling molecules of the mammalian endocannabinoid system, which comprises the cannabinoid receptors CB1 and CB2, metabolic enzymes for synthesis and degradation of the endocannabinoids, and ancillary proteins involved in receptor trafficking and modulation.[9–17]

Numerous studies in laboratory animals have established a strong link between endocannabinoid signaling and energy homeostasis, defined as the precise matching of caloric intake with energy expenditure.[18] Food deprivation increases endocannabinoid levels in the nucleus accumbens and hypothalamus, brain regions that express CB1 receptors and contribute to appetitive regulation.[19] Systemic administration of THC or endogenous cannabinoids increases feeding.[20] Micro-injection of cannabinoid receptor agonists or endocannabinoids directly into the nucleus accumbens also increases feeding.[21,22] Thus, the endocannabinoid system can be viewed as a short-latency effector system for restoring energy homeostasis under conditions of food deprivation.[18,23–25]

To respond effectively to an energy deficit, an animal should be driven to seek food (*appetitive* behavior) and, once food is encountered, to maximize caloric intake (*consummatory* behavior). The endocannabinoid system is capable of orchestrating both aspects of this response. With respect to appetitive behavior, CB1 agonists reduce the latency to feed[26–32] and induce animals to expend more effort to obtain a food or liquid reward,[30,31,33,34] whereas CB1 antagonists have the opposite effects.[26–32] As for consummatory behavior, rodent studies show that administration of THC or endocannabinoids not only increases consumption, but also alters food preferences in favor of palatable, calorically dense foods, such as those laden with sugars and fats. For example, THC causes rats to consume larger quantities of chocolate cake batter without affecting consumption of concurrently available laboratory pellets.[35] It also causes them to consume larger quantities of sugar water than plain water, and of dry pellets rather than watered-down pellet mash, which is calorically dilute.[36] Administration of endocannabinoids, systemically or directly into the nucleus accumbens, has similar effects, which can be blocked by administration of CB1 antagonists.[22,37,38] Conversely, CB1 antagonists, administered alone, specifically suppress consumption of sweet and fatty foods in rats[39–41] and primates,[42] indicating that basal CB1 activation can be regulated up or down to alter consumption.

There is experimental support for the hypothesis that cannabinoids amplify the pleasurable or rewarding aspects of calorically dense foods. This phenomenon has been termed *hedonic amplification*,[21,43] whereas the food-specific increase in consumption it engenders has been termed *hedonic feeding*.[44] Although inferences about the subjective experience of animals can be difficult to establish, cannabinoids have been shown to increase overt expressions of pleasure during feeding. In rats, for example, both THC and AEA increase the vigor of licking at spouts delivering

sweet fluids.[45,46] Further, the frequency of orofacial movements associated with highly palatable foods is increased or decreased by injection of THC or a CB1 antagonist respectively, suggesting that pleasure may be increased by cannabinoid administration.[47,48]

The effects of cannabinoids on hedonic responses may be partially chemosensory in origin, involving both taste (gustation) and smell (olfaction). With respect to gustation, a majority of sweet-sensitive taste cells in the mouse tongue are immunoreactive to CB1, and a similar proportion shows heightened responses to saccharin, sucrose, and glucose following endocannabinoid administration.[49,50] These effects are recapitulated in afferent nerves carrying gustatory signals from the tongue,[49] as administration of AEA or 2-AG specifically increases chorda tympani responses to sweeteners rather than NaCl (salt), HCl (sour), quinine (bitter), or monosodium glutamate (umami). As for olfaction, CB1 receptors expressed in the olfactory bulb are required for post-fasting hyperphagia in mice, and THC decreases the threshold for food-odor detection during exploratory behavior.[51]

The high degree of evolutionary conservation of the endocannabinoid system at the molecular level is well established.[52] Although CB1 and CB2 receptors are unique to chordates, there are numerous candidates for cannabinoid receptors in most animals. Furthermore, orthologs of the enzymes involved in synthesis and degradation of endocannabinoids occur throughout the animal kingdom. This degree of molecular conservation, coupled with the universal need in organisms to regulate energy balance, suggests the hypothesis that hedonic amplification and hedonic feeding are also widely conserved, but studies in animals other than rodents and primates appear to be lacking.

The present study tests the hypothesis that the hedonic effects of cannabinoids are conserved in the nematode *C. elegans*. This organism diverged from the lineage leading to mammals more than 500 million years ago.[53] Nevertheless, *C. elegans* has a fully elaborated endocannabinoid signaling system including:[54] (i) functionally validated endocannabinoid receptors NPR-19, which most closely resembles the mammalian CB1 receptor, and OCTR-1, and putative receptors encoded by *npr-32*, *osm-9*, and *trp-4*;[55–57] (ii) the endocannabinoids AEA and 2-AG, which it shares with mammals,[45,58–60] (iii) orthologs of the mammalian endocannabinoid synthesis enzymes NAPE-PLD and DAGL,[61] and (iv) orthologs of the endocannabinoid degradative enzymes FAAH and MAGL (Y97E10AL.2 in worms).[55] Endocannabinoid signaling in *C. elegans* is currently known to contribute to six main phenotypes: (i) axon navigation during regeneration,[56,62] (ii) lifespan regulation related to dietary restriction,[61,63] (iii) progression through developmental stages,[61,64] (iv) suppression of nociceptive withdrawal responses,[55] (v) inhibition of feeding rate,[55] and (vi) inhibition of locomotion.[55,57]

The feeding ecology of *C. elegans* supports the possibility of hedonic feeding in this organism. *C. elegans* feeds on bacteria in decaying plant matter.[65] It finds bacteria through chemotaxis guided by a combination of gustatory and olfactory cues.[66,67] Bacteria are ingested through the worm's pharynx, a rhythmically active muscular pump that constitutes the animal's throat. Although *C. elegans* is an omnivorous bacterivore, different species of bacteria have a characteristic nutritional quality as a food source defined by the growth rate of individual worms feeding on that species.[68] Hatchlings are naïve to food quality but in a matter of hours begin to exhibit a preference for

nutritionally superior species (henceforth *superior food*) over nutritionally inferior species (henceforth *inferior food*).[69]

Here we show that exposure of *C. elegans* to the endocannabinoid AEA biases both consummatory and appetitive responses toward superior food. With respect to consummatory behavior, animals exposed to AEA increase their feeding rate on superior food and decrease their feeding rate on inferior food. As for appetitive behavior, the fraction of worms approaching and dwelling on patches of superior food increases whereas the fraction approaching and dwelling on inferior food decreases. Taken together, the consummatory and appetitive manifestations of cannabinoid exposure in *C. elegans* imply increased consumption of superior food characteristic of hedonic feeding on calorically dense foods by mammals. We also find that AEA's effects require the NPR-19 cannabinoid receptor. Further, AEA's effects persist when *npr-19* gene is replaced by the human CB1 receptor-gene CNR1, indicating a high degree of conservation between the nematode and mammalian endocannabinoid systems. At the neuronal level, we find that under the influence of AEA, AWC, an olfactory neuron required for chemotaxis to food, becomes more sensitive to superior food and less sensitive to inferior food. Together, our findings indicate that the hedonic effects of endocannabinoids may be conserved in *C. elegans*.

Results

AEA exposure increases consumption of superior food

In mammals, cannabinoids can selectively increase consumption of foods that are nutritionally superior in the sense that they are calorically dense.[35,36] We asked whether cannabinoids can selectively increase consumption of nutritionally superior food in *C. elegans*, where nutritional quality is defined in terms of the growth rate of individual worms.[68] *C. elegans* swallows bacteria by rhythmically contracting its pharynx; each contraction is called a pump. To quantify consumption, we recorded pumping rate electrically in individual worms restrained in a microfluidic channel containing a single type of food (OD_{600} 0.8; Figure 1A).[70,71] We first tested the effect of AEA exposure on consumption of the bacterial strain OP50, a classical laboratory food source. As previously reported,[72] AEA exposure decreased consumption of OP50 (Figure 1A, 1B; Table S1, line 1). We then tested the effect of AEA exposure on consumption of five bacteria strains for which objective quality as a food source has been measured.[68] Baseline food consumption in unexposed worms did not correlate with nutritional quality. Nevertheless, AEA exposure increased the consumption of superior food, decreased the consumption of inferior food, and had no effect on food of intermediate quality (Figure 1C; Table S1, lines 2-6).[72] We conclude that AEA induces hedonic feeding in *C. elegans.* Furthermore, its effects on feeding are reciprocal, increasing and decreasing consumption of superior and inferior food, respectively.

AEA exposure increases appetitive responses to superior food

In mammals, cannabinoids cause a shift toward nutritionally superior food not only in consummatory behavior but also appetitive behavior, defined as the tendency to seek a particular food. We asked whether cannabinoids can selectively increase appetitive responses to nutritionally

163 superior food in *C. elegans*, measured in terms of chemotaxis preference. We began by assessing
164 changes in relative preference for the superior food DA1877 and the inferior food DA1885.
165 Preference was measured by placing a small population of worms at the start of a T-maze (Figure
166 2A) baited with patches of the two bacteria strains at equal concentration (OD_{600} 1). The T-maze
167 assay is analogous to mammalian studies in which both palatable and standard food options are
168 simultaneously available.[22,35–38] The number of worms in each food patch was counted at 15-
169 minute intervals for one hour. Preference index I at each time point was quantified as $I =$
170 $(n_S - n_I)/(n_S + n_I)$, where n_S and n_I are the number of worms on superior and inferior food,
171 respectively; $I = 0$ indicates indifference between the two food types. We pre-exposed well-fed
172 worms from the reference strain N2 to 100 µM AEA for 20 min in foodless M9 buffer. We found
173 that AEA exposure increased preference for superior food (Figure 2B, C; Table S2, line 2). This
174 effect lasted at least 60 minutes without significant decrement (Figure 2B; Table S2, lines 3-4)
175 despite the absence of AEA on the assay plates.
176
177 One interpretation of the data in Figure 2B-C is that AEA exposure specifically increases the
178 attractiveness of superior food relative to inferior food. However, an alternative interpretation is
179 that AEA promotes the attractiveness of whichever food is already preferred under the baseline
180 conditions of the experiment (AEA–). To distinguish between these possibilities, we titrated the
181 densities of superior and inferior food until, under baseline conditions, neither food was preferred
182 ($I \approx 0$; Figure 2D, E; Figure S1A, B). Under these conditions, AEA still increased the preference
183 for superior food (Table S2, lines 6, 10). This finding suggests that AEA differentially affects
184 accumulation based on food identity. We also tested the effect of AEA on preference for a second
185 pair of superior and inferior bacteria, HB101 and DA837, for which the difference in nutritional

quality is smaller than in the previous pair (Figure 2F; Figure S1C); as before, the baseline preference was titrated approximately to zero. Once again, AEA caused increased preference for superior food (Table S2, line 14). Taken together, the data in Figure 2B-F show that AEA's ability to increase preference for superior food is limited neither to a particular pair of foods nor their relative concentrations.

Because worms in the T-maze could occupy foodless regions between the food patches, the increase in preference index could represent increased attraction to superior food, decreased attraction to inferior food, or both. An increase in the preference index that resulted only from decreased attraction to inferior food would not be evidence of increased appetitive responses to superior food. However, further analysis revealed that AEA exposure increased the fraction of worms on superior food (Figure 2G; Table S2, line 18), and decreased the fraction of animals on inferior food (Figure 2G; Table S2, line 22). Thus, AEA-induced changes in appetitive responses to superior and inferior food that result in increased accumulation on superior food are consistent with the increased appetitive responses to superior food. We conclude that AEA has reciprocal actions on both appetitive and consummatory responses.

Chemosensory correlates of hedonic feeding

Accumulation in a food patch is determined by only two factors: the rates of food-patch entry and exit. AEA could modulate appetitive responses by acting on either or both rates. Chemotaxis toward food patches is driven mainly by olfactory neurons responding to distal cues.[66,67] Thus, changes in entry rate as a function of AEA exposure would imply changes in the function of olfactory neurons. We therefore added a paralytic agent[73] to both food patches in the T-maze,

thereby setting exit rate to zero. We found that AEA still produced a marked increase in preference for superior food (Figure 3A; Table S3, line 2), showing that it differentially affects patch entry rates.

We next considered the possibility that AEA acts on specific olfactory neurons to produce the appetitive component of hedonic feeding. *C. elegans* senses food-related odors by 11 classes of chemosensory neurons (two neurons/class).[67,74] We focused on AWC, a class of olfactory neurons that respond directly to many volatile odors[75] and are required for chemotaxis to them.[67] We measured AEA's effect on preference in *ceh-36* mutants, in which AWC function is impaired. The gene *ceh-36* is expressed by AWC and encodes a homeodomain transcription factor required for expression of genes essential for chemosensory transduction.[76,77] Accordingly, *ceh-36* mutants are strongly defective in chemotaxis toward food-related odors sensed by AWC.[77] *ceh-36* is also expressed in one other chemosensory neuron class, ASE, but as ASE neurons inherit their sensitivity to odorants via peptidergic signaling from AWC, loss of appetitive responses to food in *ceh-36* mutants would nevertheless be attributable to loss of AWC function. In T-maze assays comparing appetitive responses in *ceh-36* mutants and N2 worms, we found a modest strain by AEA interaction ($p = 0.08$), and a significant effect of AEA in N2 animals that was absent in the mutants (Figure 3B; Figure S2A, B; Table S3, lines 6, 10-11, 13). This finding indicates that AWC is required for the appetitive component of hedonic feeding.

AWC is activated by decreases in the concentration of food or food-related odors.[74,78,79] AWC can nevertheless promote attraction to food patches because its activation truncates locomotory head bends away from the odor source, thereby steering the animal toward it. Additionally, its activation

causes the animal to stop moving forward, reverse, and resume locomotion in a new direction better aligned with the source, a behavioral motif known as a *pirouette*.[80] To test whether AEA alters AWC sensitivity to superior and inferior foods, we compared AWC calcium transients in response to the removal of food in N2 worms exposed to AEA, and in unexposed controls. In unexposed animals, AWC neurons responded equally to the removal of either food (Figure 3C, D, Table S3, line 21). However, exposure to AEA caused a reciprocal change in food sensitivity, increasing AWC's response to the removal of superior food and decreasing its response to the removal of inferior food (Figure 3C, D, Table S3, lines 17, 19-20, 22). These reciprocal effects mirror AEA's effect on both the consummatory and appetitive aspects of hedonic feeding (Figures 1 and 2) and are consistent with a model in which hedonic feeding is triggered, at least in part, by modulation of chemosensation in AWC neurons.

Dissection of signaling pathways required for hedonic feeding

The G-protein coupled receptor NPR-19, encoded by the *C. elegans* gene *npr-19*, has been shown to be required for AEA-mediated suppression of withdrawal responses and feeding rate.[55] To test whether *npr-19* is required for hedonic feeding, we measured food preference in two deletion alleles of *npr-19* following exposure to AEA. Mutant worms failed to exhibit increased preference for superior food (Figure 4A; Figure S2C-F; Table S4, lines 6-7, 10-11). This defect was rescued by over-expressing *npr-19* under control of the native *npr-19* promoter (Figure 4A; Figure S2E, F, G; Table S4, lines 19-20, 22). We conclude that *npr-19* is required for the appetitive component of hedonic feeding. This defect was also rescued by over-expressing the human cannabinoid receptor gene CNR1 (Figure 4A; Figure S2E, F, H; Table S4, lines 28-29, 31). This finding

indicates a remarkable degree of conservation between the nematode and human endocannabinoid systems, as previously reported.[55]

The foregoing results suggest a model of hedonic feeding in *C. elegans* in which activation of the NPR-19 receptor by AEA triggers reciprocal changes in AWC's food sensitivity to induce the appetitive component of hedonic feeding. We therefore tested whether *npr-19* is required for AEA's effects on AWC. The effect of AEA on AWC's response to food was abolished in *npr-19* mutants (Figure 4B, C, Table S4, lines 34, 37-38, 43, 46-47). This phenotype was partially rescued by over-expression of *npr-19* under control of the native *npr-19* promoter (Figure S3A, B, Table S5, lines 3, 6-7,12, 15-16), and by over-expression of human cannabinoid receptor gene CNR1 (Figure S3C, D, Table S5, lines 22, 25-26, 31, 34-35). We conclude that the appetitive component of AEA-induced hedonic feeding requires both the NPR-19 receptor and AWC neurons, and that activation of the NPR-19 receptor by AEA triggers reciprocal changes in AWC's food sensitivity, contributing to increased preference for superior food.

The simplest explanation for AEA's effect on AWC would be that NPR-19 is expressed in AWC, and its activation by AEA produces the observed reciprocal modulation of AWC sensitivity to superior and inferior foods. To characterize the *npr-19* expression pattern, we expressed a p*npr-19*::GFP transgene together with either p*cho-1*::mCherry or p*eat-4*::mCherry, two markers whose neuronal expression pattern is known completely.[81,82] We observed expression of *npr-19* in approximately 29 neuron somata in the head and 8 in the tail (Figure 5A, Table S6). Using positional cues in addition to the markers, we positively identified 28 of the GFP-positive somata, which fell into 15 neuron classes (Table 1). These classes could be organized into four functional groups:

sensory neurons (URX, ASG, AWA, and PHC), interneurons (RIA, RIM, and LUA), motor neurons (URA and PDA), and pharyngeal neurons (M1, M3, MI, MC, I2, and I4). Although AWC could be identified in every worm by its characteristic position in the p*eat-4*::mCherry expressing strain, co-expression of p*npr-19*::GFP transgene was not observed in this neuron class. Our expression data, together with the absence of significant *npr-19* expression in AWC in RNA sequencing experiments based on the *C. elegans* Neuronal Gene Expression Map & Network (CeNGEN) consortium,[83] suggests that AWC does not express *npr-19*. These findings are inconsistent with a direct model of action of AEA on AWC neurons mediated by the NPR-19 receptor.

The *npr-19* expression pattern supports two possible indirect models of AEA's effect on AWC. In the first model, AWC inherits its sensitivity to AEA from AEA-sensitive synaptic pathways that involve classical neurotransmitters; this mechanism is plausible because cannabinoid signaling is known to inhibit release of classical neurotransmitters in mammals.[84] In the second model, AWC inherits its sensitivity from AEA-sensitive signaling pathways that involve neuromodulators[85]. To test whether classical synaptic pathways render AWC sensitive to AEA, we imaged AWC activity in worms with a null mutation in *unc-13*, the *C. elegans* homolog of Munc13, which is required for exocytosis of the clear-core synaptic vesicles that contain classical neurotransmitters.[86] In *unc-13* mutants, exposure to AEA caused a reciprocal change in food sensitivity, just as in N2. (Figure 5B, C; Table S7, lines 3, 6-7, 9, 13, 15-16, 18). This result makes it unlikely that AWC inherits its AEA sensitivity from synaptic pathways that involve classical neurotransmitters.

We next investigated the model in which AEA causes the release of neuromodulators that might act on AWC. Most neuromodulatory substances, such as neuropeptides and biogenic amines, are

300 released by exocytosis of dense-core vesicles.[87,88] Gene expression data[83] indicate that most of the
301 *npr-19*-expressing neurons also express *unc-31* (11 out of 15, Table 1),[89] the *C. elegans* ortholog
302 of human CADPS/CAPS, a gene required for exocytosis of dense-core vesicles. This
303 correspondence provides an anatomical substrate for cannabinoid-mediated release of
304 neuromodulators. We therefore recorded from AWC in an *unc-31* deletion mutant. If AEA's effect
305 on AWC were solely the result of neuromodulation mediated by *unc-31*, one would expect this
306 mutation to phenocopy *npr-19* null, exhibiting no AEA effects on AWC responses. This appeared
307 to be the case for the response to superior food, in which there was no effect of AEA (Figure 5D,
308 E; Table S7, lines 21, 24-25, 27). Although AWC responses to inferior food were still modulated
309 by AEA, they were increased rather than decreased (Figure 5D, E; Table S7, lines 31, 33, 36). We
310 conclude that AEA's modulation of AWC food sensitivity is severely disrupted in *unc-31* mutants.
311 We cannot rule out the possibility that overall disruption of neuromodulation in *unc-31* mutants
312 results in non-specific developmental or functional disruption in AWC physiology. Nevertheless,
313 the phenotypes of *unc-13* and *unc-31* taken together support a model in which NPR-19 receptors
314 activated by AEA promote the release of dense-core vesicles containing modulatory substances
315 that act on AWC (Figure 6).
316

Discussion

In mammals, administration of THC or endocannabinoids induces hedonic feeding. The present study provides two converging lines of evidence supporting the hypothesis that cannabinoids induce hedonic feeding in *C. elegans*. First, in the five bacteria strains for which food quality has previously been characterized,[68] AEA reciprocally altered food consumption, causing worms to feed at higher and lower rates on superior food and inferior food, respectively (Figure 1C), with no effect on a food of intermediate quality. We found that this trend extends to a sixth strain, OP50, whose quality as a food source was not previously characterized but is likely to be an inferior food,[90,91] as its consumption was suppressed by AEA, as previously reported (Figure 1B).[55] In the second line of evidence, AEA can differentially alter appetitive behavior. AEA exposure causes increased preference for superior food, which can be traced to a larger proportion of worms accumulating on superior food and smaller proportion accumulating on inferior food (Figure 2G). In the T-maze assay, individual worms are capable of exiting one patch and entering the other multiple times over the duration of the experiments.[69] Thus, the proportions of worms accumulating in each patch are mathematically equivalent to the average *fraction of time* that an individual worm spends feeding in each patch. Therefore, even if worms were feeding at the same rate in the two patches, consumption of superior food would be increased under the influence of AEA. We can therefore infer that the effect of AEA on accumulation is further evidence of increased consumption of superior food. Together, these findings support the conclusion that AEA induces hedonic feeding in *C. elegans*.

Our findings confirm and extend previous investigations concerning the role of the endocannabinoid system in regulating feeding in *C. elegans.* We confirmed expression of *npr-19* in the inhibitory pharyngeal motor neuron M3 and the sensory neuron URX.[55] We extended these results by identifying 13 additional *npr-19* expressing neurons, including sensory neurons, interneurons, and motor neurons. Of particular interest is the detection of *npr-19* expression in five additional pharyngeal neurons. Thus, 6 of the 20 neurons comprising the pharyngeal nervous system are potential sites for endocannabinoid mediated regulation of pumping rate. Interestingly, these 6 neurons include the motor neuron MC, the pacemaker regulating pharyngeal pumping frequency,[92,93] and M3, which regulates pump duration.[94] It will now be illuminating to investigate the neuronal mechanism underlying reciprocal modulation of pumping rate in response to superior and inferior foods.

To date, only a small number of studies have examined the effects of cannabinoids on feeding and food preference in invertebrates. Early in evolution, the predominant effect may have been feeding inhibition. For example, cannabinoid exposure shortens bouts of feeding in Hydra[95] and larvae of the tobacco hornworm moth *Manduca sexta* prefer to eat leaves containing lower rather than higher concentrations of the phytocannabinoid cannabidiol.[96] In adult fruit flies (*Drosophila melanogaster*), exposure to phyto- or endocannabinoids (AEA and 2-AG) for several days before testing reduces consumption of standard food.[97] On the other hand, in side-by-side tests of sugar-yeast solutions with and without added phyto- or endocannabinoids, flies prefer the cannabinoid-spiked option. The picture that emerges is that whereas the original response to cannabinoids may have

been feeding suppression, through evolution the opposite effect arose, sometimes in the same organism. As we have shown, *C. elegans* exhibits both increases and decreases in consummatory and appetitive responses under the influence of cannabinoids.

Although administration of cannabinoids causes hedonic feeding in *C. elegans* and mammals, there are notable differences in how it is expressed. One experimental design commonly used in mammalian studies is to measure consumption of a single test food, which is either standard laboratory food or calorically dense food. In such experiments, consumption of both types of food is increased following cannabinoid system activation.[20,98,99] The analogous experiment in the present study is the experiment of Figure 1, in which consumption was measured in response to different foods presented alone, ranging from nutritionally superior to inferior. We found that consumption of superior food increases as in mammalian studies whereas, in contrast, consumption of inferior food decreases. A second experimental design commonly used in mammalian studies is to measure consumption of standard and calorically dense foods when both options are simultaneously available. In this type of experiment, cannabinoids increase consumption of calorically dense food, but consumption of standard food is unchanged.[22,35–38] Cannabinoid receptor antagonists produce the complementary effect: reduced consumption of calorically dense food with little or no change in consumption of standard food.[40,41] The analogous experiments in the present study are the T-maze assays in which maze arms are baited with superior and inferior food. We find that following cannabinoid administration, consumption of superior food increases whereas consumption of inferior food decreases.

Considering both experimental designs, cannabinoids in *C. elegans* have reciprocal effects on consumption, whereas in mammals this appears not to be the case. It is conceivable that reciprocal responses are energetically advantageous in that they produce a stronger bias in favor of superior food than a unidirectional response, raising the question of why reciprocal responses have not been reported in mammals. There are, of course, considerable differences in the feeding ecology of nematodes and mammals, possibly making unidirectional responses a better strategy in mammals. On the other hand, differences in experimental procedures may explain the absence of reciprocal responses in mammals. In mammalian studies in which the two foods are presented together, standard and calorically dense foods are placed in close proximity such that there is essentially no cost in terms of physical effort for the animal to switch between feeding locations. It is conceivable that increasing the switching cost[100] could lead to a differential effect on consumption in mammals.

We propose the following model of differential accumulation on food leading to hedonic feeding in *C. elegans* (Figure 6). The model focuses on the olfactory neuron AWC, which is necessary and sufficient for navigation to the source of food-related odors[101] and whose responses exhibit reciprocal modulation by AEA. In mammals, cannabinoids have been observed to modify chemosensitivity in the periphery and brain. Both AEA and 2-AG amplify the response of primary chemosensory cells, such as sweet-taste cells in the tongue,[49,50] which might explain increased consumption of sweet foods and liquids. Cannabinoids can also increase the sensitivity of the mammalian central olfactory system during food-odor exploration.[51,102,103] We found that AEA alters the sensitivity of the olfactory neuron AWC. In unexposed worms, AWC is equally sensitive to superior and inferior food, suggesting it cannot detect a difference in the odors released by the two food types. However, in remarkable alignment with the reciprocal changes we observed in consumption, AEA

makes this neuron more sensitive and less sensitive to superior food and inferior food, respectively. Previous studies have demonstrated that activating AWC, by decreasing attractant concentration or by exogenous activation, triggers reorientation toward attractants.[101,104–106] The increased response of AWC to removal of superior food triggered by AEA likely enhances reorientation toward such food; conversely, the decreased response to removal of inferior food likely weakens reorientation to such food. The requirement for *ceh-36* in rendering *C. elegans* food preferences sensitive to AEA suggests that AWC neurons provide a link between AEA and hedonic feeding. However, we do not exclude the possibility of contributions from other chemosensory neurons. Of particular interest are the two chemosensory neurons AWA and ASG, both of which express *npr-19* and are required for chemotaxis.[66,67] It will now be important to map cannabinoid sensitivity across the entire population of food-sensitive neurons to understand how cannabinoids alter the overall chemosensory representation of superior and inferior foods.

AEA's effect on AWC appears to be indirect. Our results are consistent with a model in which AEA activates NPR-19 receptors to promote release of dense-core vesicles containing neuromodulators that act on AWC. This model is supported by evidence in *C. elegans* that 2-AG, which activates NPR-19, stimulates widespread release of serotonin;[55,57] therefore, NPR-19 activation seems capable of promoting dense-core vesicle release. Additionally, AWC expresses receptors for biogenic amines and responds to neuropeptides released by neighboring neurons,[107,108] suggesting that it has postsynaptic mechanisms for responding to various neuromodulators. Identification of one or more neuromodulators responsible for AEA's effect on AWC, together with their associated receptors, will help answer the question of how AEA causes reciprocal changes in food-odor sensitivity.

Our results establish a new role for endocannabinoids in *C. elegans*: the induction of hedonic feeding. The endocannabinoid system and its molecular constituents offer significant prospects for pharmacological management of health, including eating disorders and substance abuse.[109] Clear parallels between the behavioral, neuronal, and genetic basis of hedonic feeding in *C. elegans* and mammals establish the utility of this organism as a new genetic model for the investigation of molecular and cellular bases of these and related disorders.

Acknowledgements

We thank Richard Komuniecki for the *npr-19*(ok2068) and rescue strains, and David Raizen for providing the DA1881 (*B. cereus*) bacterial strain. The *unc-13, unc-31, ceh-36, cho-1*, and *eat-4* worm strains were provided by the CGC, which is funded by the NIH Office of Research Infrastructure Programs (P40 OD010440). We thank Oliver Hobert, Jonathan Millet, and Jon Pierce for discussion, and Leon Avery and Matthew Smear for comments on the manuscript. We thank Chris Doe for use of a Zeiss LSM800 confocal microscope for imaging. Funding for this project was provided by NIDA (DA047645) and NIGM (GM129576).

Author contributions

Conceptualization: S.R.L.; Data curation: A.L., S.F.; Formal Analysis: A.L., S.F.; Funding acquisition: S.R.L.; Investigation: A.L., S.F., R.Z.B., Z.P., A.M.W., K.C; Methodology: A.L., S.F., S.R.L.; Project administration: S.R.L.; Supervision: A.L., S.F., K.C., S.R.L.; Validation: S.F., A.L., A.M.W., K.C.; Visualization: A.L., S.F., S.R.L.; Writing – original draft: A.L., S.F., S.R.L.; Writing – review & editing: A.L., S.F., S.R.L.

Inclusion and diversity statement

We support inclusive, diverse, and equitable conduct of research.

Declaration of Interests

Shawn R. Lockery is co-founder and Chief Technology Officer of InVivo Biosystems, Inc., which manufactures instrumentation for electrophysiological recording of pumping rate in nematodes and is the author of the patent Electropharyngeogram arrays and methods of use (US-9723817-B2). The other authors have no competing interests.

463 **Figure titles and legends**

464 **Figure 1. AEA-mediated hedonic feeding: consummatory behavior. A.** Electrical recordings
465 of pharyngeal pumping in two individual worms under the conditions shown. Each spike is the
466 electrical correlate of one pharyngeal pump. Traces are representative of the median pumping
467 frequency under each condition. **B.** Effect of AEA on mean pumping frequency in OP50 (OD 0.8).
468 **C.** Effect of AEA on mean pumping frequency in five different bacteria species (OD 0.8). Pairs of
469 bars are ordered (left to right) according to growth rate of *C. elegans*, defined as the inverse of the
470 number of days to grow from L1 to adult, when cultivated on the corresponding bacteria; each
471 growth rate value is the mean of four test conditions in previously published work. Gray bars,
472 AEA–. Black bars, AEA+. Red lines, median pumping frequency. For details of statistics see Table
473 S1. Symbols, *, $p < 0.05$; **, $p < 0.01$; ***, $p < 0.001$; n.s., not significant. Error bars, 95%
474 confidence interval. Number of recorded worms is shown in parentheses.
475
476 **Figure 2. AEA-mediated hedonic feeding: appetitive behavior. A.** Food preference assay. T-
477 maze arms were baited with patches of superior (blue) and inferior (orange) bacteria. **B.** Mean
478 preference index (I) versus time for AEA-exposed animals (AEA+) and unexposed controls
479 (AEA–), where $I > 0$ is preference for superior food, $I < 0$ is preference for inferior food, and $I =$
480 0 is indifference (dashed line). Superior food, DA1877, OD_{600} 1; inferior food, DA1885, OD_{600} 1.
481 **C.** Summary of the data in B. Each dot is mean preference over time in a single T-maze assay. Dot
482 color indicates preference index according to the color scale on the right. **D, E.** Effect of AEA on
483 preference when baseline preference is statistically indistinguishable from the indifference point
484 (symbols and color scale as in C). For preference time courses, see Figure S1A, B. In D: Superior
485 food, DA1877, OD_{600} 0.5; inferior food, DA1885, OD_{600} 3. In E: superior food, DA1877, OD_{600}

0.5; inferior food, DA1885, OD_{600} 8. **F.** Effect of AEA on preference for a different pair of superior and inferior bacteria. Superior food, HB101, OD_{600} 0.5; inferior food, DA837, OD_{600} 2.2 (symbols and color scale as in C). For preference time course, see Figure S1C. **G.** Effect of AEA on fraction of worms in superior and inferior food patches versus time. Same experiment as in panels B, C. For statistics see Table S2. Symbols: *, $p < 0.05$; **, $p < 0.01$; ***, $p < 0.001$; n.s., not significant. Error bars, 95% confidence interval.

Figure 3. Chemosensory correlate of hedonic feeding. A. Mean preference index (I) versus time for AEA-exposed animals (AEA+) and unexposed controls (AEA–) when sodium azide was added to food patches. Superior food, DA1877, OD_{600} 0.5; inferior food, DA1885, OD_{600} 3. **B.** Effect of AEA on preference in N2 and *ceh-36* mutants. Superior food, DA1877, OD_{600} 0.5; inferior DA1885, OD_{600} 8. Each dot is mean preference in a single T-maze assay. For preference time course, see Figure S2A, B. **C.** Effect of AEA on the amplitude of AWC calcium transients in response to the removal of superior or inferior food in N2 worms. Each trace is average normalized fluorescence change ($\Delta F/F$) versus time. Superior food (blue), DA1877, OD_{600} 1; inferior food (orange), DA1885, OD_{600} 1. **D.** Summary of the data in C, showing mean peak $\Delta F/F$. For statistics in A-D, see Table S3. Symbols: *, $p < 0.05$; **, $p < 0.01$; n.s., not significant. Error bars and shading, 95% confidence interval.

Figure 4. Requirement of NPR-19 for hedonic feeding and chemosensory modulation. A. Effect of AEA on preference in N2 worms and the indicated genetic background. Separate N2 control groups were used for *npr-19*(tm2574) vs and *npr-19*(ok2068) and rescue strains as these two sets of experiments were not contemporaneous. Superior food, DA1877, OD_{600} 0.5; inferior

food, DA1885, OD_{600} 8. Each dot is mean preference over time in a single T-maze assay. Dot color indicates preference index according to the color scale on the right. For preference time course, see Figure S2. **B.** Effect of AEA on amplitude of AWC calcium transients in response to the removal of superior or inferior food in *npr-19*(ok2068). Each trace is average normalized fluorescence change ($\Delta F/F$) versus time. Superior food (blue), DA1877, OD_{600} 1; inferior food (orange), DA1885, OD_{600} 1. **C.** Summary of the data in B, showing mean peak $\Delta F/F$. See also Figure S3 and Table S5. For statistics in A-C, see Table S4. Symbols: *, $p < 0.05$; **, $p < 0.01$; n.s., not significant. Error bars and shading, 95% confidence interval.

Figure 5. Genetic pathways underlying AEA-mediated AWC modulation. A. Expression pattern of *npr-19* in head and tail neurons. *npr-19* expression is shown in green. Left, *eat-4* expression, labeling glutamatergic neurons, is shown in magenta. Dashed circle, the soma of AWC, which is glutamatergic. Right, *cho-1* expression, labeling cholinergic neurons, is shown in magenta. Top, bottom, head and tail expression, respectively. **B.** Effect of AEA on amplitude of AWC calcium transients in response to the removal of superior or inferior food in *unc-13* null mutants. Each trace is average normalized fluorescence change ($\Delta F/F$) versus time. Superior food (blue), DA1877, OD_{600} 1; inferior food (orange), DA1885, OD_{600} 1. **C.** Summary of the data in B, showing mean peak $\Delta F/F$. **D.** Effect of AEA on amplitude of AWC calcium transients in response to the removal of superior or inferior food in *unc-31* null mutants. Each trace is average normalized fluorescence change ($\Delta F/F$) versus time. Superior food (blue), DA1877, OD_{600} 1; inferior food (orange), DA1885, OD_{600} 1. **E.** Summary of the data in D, showing mean peak $\Delta F/F$. See also Table S6. For statistics in B-E, see Table S7. Symbols: *, $p < 0.05$; **, $p < 0.01$; n.s., not significant. Error bars and shading, 95% confidence interval.

Figure 6. A model for AEA-induced hedonic feeding. AEA binds to NPR-19 on a neuron upstream of AWC, releasing dense-core vesicle release containing neuromodulators. These neuromodulators increase AWC's activation in response to superior food removal and, conversely, decreases AWC's activation in response to inferior food removal. As AWC causes worm attraction to, and retention in food patches, this bidirectional modulation leads to increased aggregation of worms on superior food and decreased aggregation on inferior food.

Tables

Table 1. *npr-19*-expressing neurons. The *npr-19* expression pattern was characterized by expressing a p*npr-19*::GFP transgene together with either p*cho-1*::mCherry or p*eat-4*::mCherry, labeling cholinergic and glutamatergic neurons, respectively.[81,82] GFP-positive neurons that expressed neither of the markers were identified by position and morphology, and confirmed by cross-reference to CeNGEN expression data showing *npr-19*. Neurotransmitter identity and *unc-31* expression of each identified neuron class are shown for comparison.[83,85] See also Table S6.

STAR methods

Resource availability

Lead contact

Requests for strains, information or datasets should be directed to the lead contact, Shawn R. Lockery (shawn@uoregon.edu).

Materials availability

Strains and plasmids generated in this study are available upon request to the lead contact.

Data and code availability

- All datasets will be shared by the lead contact upon request.
- This paper does not report original code.
- Any additional information required to reanalyze the data reported in this paper is available from the lead contact upon request.

Experimental model and subject details

Strains. Animals were cultivated under standard conditions[111] using *E. coli* OP50 as a food source. Young adults of the following strains were used in all experiments: (see Key Resources Table for details): N2, Bristol (Reference strain), FK311, RB1668, C02H7.2(tm2574), XL324, XL325 (Preference and feeding assays), XL322, XL327, XL326, XL346, XL348 (Calcium imaging), XL334, XL335 (*npr-19* expression pattern).

Bacteria. The following bacterial strains were used in this study (see Key Resources Table for details): DA1885 (*Bacillus simplex*), DA1877 (*Comamonas sp*.), *E. Coli* HB101, *E. Coli* DA837,

E. Coli OP50 and DA1881 (S13, *Bacillus cereus*). Bacteria were grown overnight at 37˚C (in presence of 50 mg/mL streptomycin for streptomycin-resistant strains: DA1877, DA1885, HB101).

Method details

Bacteria preparation. Bacteria were concentrated by centrifugation, rinsed three times with either M9 buffer (for EPG experiments) or A0 buffer (for behavioral/imaging experiments; MgSO4 1 mM, CaCl2 1 mM, HEPES 10 mM, glycerol to 350 mOsm, pH 7.1), and resuspended to their final concentration. Concentration was defined as optical density at 600 nm (OD_{600}), as measured with a DSM cell density meter (Laxco, Bothell, WA, USA). All measurements were performed on samples diluted into the linear range of the instrument (OD_{600} 0.1-1). Previous experiments determined that OD_{600} 1 corresponds to approximately 2.35 × 109 and 2.00 × 109 colony forming units/mL of *Comamonas* and *B. Simplex*, respectively (Katzen et al., 2021).

Animal preparation. Worms were washed five times in M9 buffer for EPG experiments or A0 buffer (see above) for behavioral/imaging experiments. Worms were then incubated for 20 minutes with either buffer alone (A0 for behavioral/imaging experiments, M9 for EPG pumping-rate assays) or buffer + 300 μM (pumping-rate assays) or 100 μM (behavioral/imaging experiments) Arachidonoylethanolamide (AEA, Cayman Chemical, Ann Arbor, MI, USA). The incubation time and relatively high concentration reflects the low permeability of the *C. elegans* cuticle to many exogenous molecules.[112,113] We based our AEA concentrations on a previous study that shows the concentration dependence of AEA effects on pharyngeal pumping rate.[55] In pilot experiments for pumping-rate and T-maze assays, we used lower AEA doses (100 μM and 50 μM,

591 respectively). As these experiments revealed small, variable effects, we chose the higher
592 concentration given above, which are still within the effective range.[55]
593
594 ***Behavioral assays***. Freshly poured NGM agar plates were dried in a dehydrator for 45
595 minutes at 45°C. A maze cut from foam sheets (Darice, Strongsville, OH, USA) using a laser cutter
596 or a cutting machine (Cricut, South Jordan, UT, USA) was placed on each plate (Figure 2A). Maze
597 arms were seeded with 4.5 μL of bacteria. Animals were deposited at the starting point of the maze
598 by liquid transfer and a transparent plastic disc was placed over the maze to eliminate air currents;
599 12 plates were placed on a flatbed scanner and simultaneously imaged every 15 minutes.[114,115] The
600 number of worms in the two patches of food and the region between them was counted manually
601 and a preference index *I* calculated as: $I = (n_S - n_I)/(n_S + n_I)$, where n_S is the number of worms
602 in the superior food patch, and n_I is the number of worms in the inferior food patch. Worms that
603 did not leave the starting point were excluded. For experiments involving mutants, a cohort of N2
604 animals was run in parallel on the same day. In some experiments, a paralytic agent (sodium azide,
605 NaN_3, 3 μL at 20 mM), was added to each food patch to prevent animals from leaving the patch
606 of food after reaching it. Sodium azide diffuses through the agar over time and its action is not
607 instantaneous. These two characteristics resulted in some worms becoming paralyzed around
608 rather than in the patch of food, as they stop short of the patch or escape the patch briefly before
609 becoming paralyzed. To account for these effects all worms within 5 mm of the end of the maze's
610 arm, rather than on food, were used when calculating preference index.
611

Pumping rate assays. Pharyngeal pumping was measured electrophysiologically using a ScreenChip microfluidic system (InVivo Biosystems, Eugene, OR, USA).[71] Following pre-incubation as described above (*Animal preparation*), worms mixed with bacterial food (OD_{600} 0.8) ±AEA 300 μM were loaded into the worm reservoir of a microfluidic device; this food density was chosen to reduce possible ceiling effects on pumping rate modulation by AEA. Individual worms were resident in the reservoir for 5-55 min. prior to being recorded; they were presumably feeding, and gaining food experience, during this time. To record voltage transients associated with pharyngeal pumping,[70] worms were transferred one at a time from the reservoir to the recording channel. Worms were given three minutes to acclimate to the channel before being recorded for one minute. Mean pumping frequency was extracted using custom code written in Igor Pro (Wavemetrics, Lake Oswego, OR, USA).

Calcium imaging. After pre-incubation with buffer (A0) or buffer +AEA (*Animal preparation*), worms were immobilized in a custom microfluidic chip and presented with alternating 30-second epochs of buffer and bacteria (either *B. Simplex* or *Comamonas sp.* at OD_{600} 1, at a flow rate of 100 μL/min) for 3 minutes. Optical recordings of GCaMP6-expressing AWC neurons were performed on a Zeiss Axiovert 135, using a Zeiss Plan-Apochromat 40X oil, 1.4 NA objective, a X-Cite 120Q illuminator, a 470/40 excitation filter, and a 560/40 emission filter. Neurons were imaged at 3-10 Hz on an ORCA-ERA camera (Hamamatsu Photonics). Images were analyzed using custom code written in MATLAB: the change in fluorescence in a hand-drawn region of interest that contained only the soma and neurite. Data were normalized to the average fluorescence F_o computed over the 15 second interval before the first food stimulus. We computed normalized fluorescence change as $\Delta F(t)/F_o$, where $\Delta F(t) = F(t) - F_o$; following convention, we

refer to this measure as "$\Delta F/F$." For comparison of treatment groups, we used the peak amplitude of post-stimulus $\Delta F/F$. In some animals, AWC appeared not to respond to the food stimulus, regardless of treatment group. To classify particular AWC neurons as responsive or non-responsive, we obtained the distribution of peak $\Delta F/F$ values in control experiments in which the stimulus channel contained no food; responsive neurons were defined as those whose peak $\Delta F/F$ value exceeded the 90th percentile of this distribution. Critically, the percentage of non-responders did not vary between AEA-treated and non-treated animals (25.46% vs 22.49% respectively; $\chi^2(1,759) = 0.699$, $p = 0.4031$).

Expression profile for npr-19. Worms were immobilized with 10 mM sodium azide (NaN_3) and mounted on 5% agarose pads formed on glass slides. Image stacks (30-80 images) were acquired using a Zeiss confocal microscope (LSM800, ZEN software) at 40X magnification. Identification of neurons was done based on published expression profiles of the p*cho-1*::mCherry[82] and p*eat-4*::mCherry[81] transgenes in *C. elegans*. Individual neurons were identified by mCherry expression and the relative positions of their cell bodies; *npr-19* expression was visualized using a p*npr-19*::GFP transgene. Co-expression of GFP and mCherry was assessed by visual inspection using 3D image analysis software Imaris (Oxford Instruments). Representative images (Figure 5) are maximum intensity projections of 30-80 frames computed using ImageJ software.[116] Expression of the NPR-19 receptor was widespread in body wall muscles but restricted to 29 neurons in the head (27 - 31, 95% confidence interval, n = 20 worms imaged) and 8 neurons in the tail (7.8 - 8.5, 95% confidence interval, n = 22 worms imaged) (Table S7). Overall, 28 of the *npr-19*-expressing neurons co-localized with either *cho-1* or *eat-4*, whereas ~9 did not co-localize with either marker. The identity of cells that did not co-localize with *cho-1* or *eat-4* was ascertained

based on cell body position and morphology, and verified by *npr-19* expression (threshold = 2) as reported in the *C. elegans* Neuronal Gene Expression Map & Network (CeNGEN) consortium database.[83]

Quantification and statistical analysis

A detailed description of statistical tests used and their results is presented in Tables S1-S6. Data were checked for normality with a Kolmogorov-Smirnov test.

Number of replicates. The minimal sample size for the T-maze assays were based on pilot experiments which demonstrated the ability to detect moderate to small effect sizes with ~10-30 replicates per experimental condition. Previously published EPG data showed that mutants/treatments could be distinguished with ~10 replicates. In order to ensure detection of small effect size across experimental conditions, ~70 to 120 replicates were performed in EPG experiments. Similarly, the minimal number of replicates for imaging experiments were based on previously published data.

Effect sizes. Effect sizes were computed as follow: Cohen's d for t-tests, partial eta-squared for ANOVAs, and $|z|/\sqrt{n}$ for Mann-Whitney test, where z is the z-score and n is the number of observations.

Behavioral experiments (T-mazes). Preference indices were analyzed using a two-factor ANOVA with repeated measures (effect of AEA by effect of time, with time as a repeated measure). For easier presentation, an average index across the four time-points was calculated and

displayed (Figure 2C-F, 3B, 4A). All timeseries are nonetheless available for inspection in Figure 2, 3A and Figure S1 and S2. The effect of AEA was deemed significant if main effect of AEA was significant in the ANOVA. Averaging the four time points in a series would only be problematic if there was a non-ordinal interaction AEA by time. Inspection of ANOVA results and time series reveal that the only AEA by time interactions are ordinal and minimal (Figure S1, S2). In cases where the effect of time was important (Figure 3A) or the interaction AEA by time was meaningful (Figure 2G) the time series of preference indices was presented. The comparison of preference indices between N2 and mutants relied on a two-factor ANOVA (effect of strain by effect of AEA). The average preference index across the four time-points was used for the comparison. In addition to an ANOVA, planned comparisons were incorporated in the experimental design using *t*-tests and focusing on four scientifically relevant contrasts: (1) mutants, AEA– vs AEA+; (2) N2, AEA– vs AEA+; (3) AEA–, mutants vs N2; (4) AEA+, mutants vs N2.

Pumping rate assay. As the data were not normally distributed in most of the cohorts, a non-parametric test (Mann-Whitney) was used to compared pumping frequencies between strains/treatments.

Calcium imaging. Peak ΔF/F was used as the primary measure. A two-factor ANOVA (effect of AEA by effect of bacteria type) was used to assess the effect of AEA on AWC responses. Planned *t*-tests were focused on four contrasts: (1) superior food, AEA– vs AEA+; (2) inferior food, AEA– vs AEA+; (3) AEA-, superior food vs inferior food; (4) AEA+, superior food vs inferior food. For comparisons between N2 and mutants, a two-factor ANOVAs (effect of AEA by effect of strain) was performed for each of the bacteria type (superior and inferior) and followed

by four contrasts (*t*-tests): (1) mutants, AEA– vs AEA+; (2) N2, AEA– vs AEA+; (3) AEA–, mutants vs N2; (4) AEA+, mutants vs N2.

Multiple comparisons. No correction for multiple comparisons was applied in *t*-tests used in pair-wise comparisons of means in multifactor experiments as the experimental design in this study relied on a small number (3 per condition) of planned (*a priori*), rather than unplanned (a posteriori), scientifically relevant contrasts.[117]

References

1. Abel, E.L. (1971). Effects of marijuana on the solution of anagrams, memory and appetite. Nature *231*, 260–261. 10.1038/231260b0.
2. Kirkham, T.C., and Williams, C.M. (2001). Endogenous cannabinoids and appetite. Nutr. Res. Rev. *14*, 65–86. 10.1079/NRR200118.
3. Foltin, R.W., Brady, J. V., and Fischman, M.W. (1986). Behavioral analysis of marijuana effects on food intake in humans. Pharmacol. Biochem. Behav. *25*, 577–582. 10.1016/0091-3057(86)90144-9.
4. Abel, E.L. (1975). Cannabis: Effects on hunger and thirst. Behav. Biol. *15*, 255–281. 10.1016/S0091-6773(75)91684-3.
5. Tart, C.T. (1970). Marijuana Intoxication : Common Experiences. Nat. 1970 2265247 *226*, 701–704. 10.1038/226701a0.
6. Halikas, J., Goodwin, D., and Guze, S. (1971). Marihuana effects. A survey of regular users. JAMA *217*, 692–694. 10.1001/JAMA.217.5.692.
7. Hollister, L.E. (1971). Hunger and appetite after single doses of marihuana, alcohol, and dextroamphetamine. Clin. Pharmacol. Ther. *12*, 44–49. 10.1002/CPT197112144.
8. Foltin, R.W., Fischman, M.W., and Byrne, M.F. (1988). Effects of smoked marijuana on food intake and body weight of humans living in a residential laboratory. Appetite *11*, 1–14. 10.1016/S0195-6663(88)80017-5.
9. Bauer, M., Chicca, A., Tamborrini, M., Eisen, D., Lerner, R., Lutz, B., Poetz, O., Pluschke, G., and Gertsch, J. (2012). Identification and quantification of a new family of peptide endocannabinoids (Pepcans) showing negative allosteric modulation at CB1 receptors. J. Biol. Chem. *287*, 36944–36967. 10.1074/JBC.M112.382481.

10. Fu, J., Bottegoni, G., Sasso, O., Bertorelli, R., Rocchia, W., Masetti, M., Guijarro, A., Lodola, A., Armirotti, A., Garau, G., et al. (2011). A catalytically silent FAAH-1 variant drives anandamide transport in neurons. Nat. Neurosci. *15*, 64–69. 10.1038/NN.2986.

11. Kaczocha, M., Glaser, S.T., and Deutsch, D.G. (2009). Identification of intracellular carriers for the endocannabinoid anandamide. Proc. Natl. Acad. Sci. *106*, 6375–6380. 10.1073/PNAS.0901515106.

12. Oddi, S., Fezza, F., Pasquariello, N., D'Agostino, A., Catanzaro, G., De Simone, C., Rapino, C., Finazzi-Agrò, A., and Maccarrone, M. (2009). Molecular identification of albumin and Hsp70 as cytosolic anandamide-binding proteins. Chem. Biol. *16*, 624–632. 10.1016/J.CHEMBIOL.2009.05.004.

13. Kaczocha, M., Vivieca, S., Sun, J., Glaser, S.T., and Deutsch, D.G. (2012). Fatty acid-binding proteins transport N-acylethanolamines to nuclear receptors and are targets of endocannabinoid transport inhibitors. J. Biol. Chem. *287*, 3415–3424. 10.1074/JBC.M111.304907.

14. Liedhegner, E.S., Vogt, C.D., Sem, D.S., Cunningham, C.W., and Hillard, C.J. (2014). Sterol carrier protein-2: binding protein for endocannabinoids. Mol. Neurobiol. *50*, 149–158. 10.1007/S12035-014-8651-7.

15. Martini, L., Waldhoer, M., Pusch, M., Kharazia, V., Fong, J., Lee, J.H., Freissmuth, C., and Whistler, J.L. (2007). Ligand-induced down-regulation of the cannabinoid 1 receptor is mediated by the G-protein-coupled receptor-associated sorting protein GASP1. FASEB J. *21*, 802–811. 10.1096/FJ.06-7132COM.

16. Rozenfeld, R., and Devi, L.A. (2008). Regulation of CB1 cannabinoid receptor trafficking by the adaptor protein AP-3. FASEB J. *22*, 2311–2322. 10.1096/FJ.07-102731.

17. Jin, W., Brown, S., Roche, J.P., Hsieh, C., Celver, J.P., Kovoor, A., Chavkin, C., and Mackie, K. (1999). Distinct domains of the CB1 cannabinoid receptor mediate desensitization and internalization. J. Neurosci. *19*, 3773–3780. 10.1523/JNEUROSCI.19-10-03773.1999.

18. Cristino, L., Becker, T., and Di Marzo, V. (2014). Endocannabinoids and energy homeostasis: An update. BioFactors *40*, 389–397. 10.1002/BIOF.1168.

19. Kirkham, T.C., Williams, C.M., Fezza, F., and Di Marzo, V. (2002). Endocannabinoid levels in rat limbic forebrain and hypothalamus in relation to fasting, feeding and satiation: stimulation of eating by 2-arachidonoyl glycerol. Br. J. Pharmacol. *136*, 550. 10.1038/SJ.BJP.0704767.

20. Williams, C.M., and Kirkham, T.C. (1999). Anandamide induces overeating: Mediation by central cannabinoid (CB1) receptors. Psychopharmacology (Berl). *143*, 315–317. 10.1007/s002130050953.

21. Mahler, S. V, Smith, K.S., and Berridge, K.C. (2007). Endocannabinoid Hedonic Hotspot for Sensory Pleasure: Anandamide in Nucleus Accumbens Shell Enhances 'Liking' of a Sweet Reward. Neuropsychopharmacology *32*, 2267–2278. 10.1038/sj.npp.1301376.

22. Deshmukh, R.R., and Sharma, P.L. (2012). Stimulation of accumbens shell cannabinoid CB1 receptors by noladin ether, a putative endocannabinoid, modulates food intake and dietary selection in rats. Pharmacol. Res. *66*, 276–282. 10.1016/J.PHRS.2012.06.004.

23. Parker, L. (2017). Cannabinoids and the Brain (The MIT Press).

24. Munro, S., Thomas, K.L., and Abu-Shaar, M. (1993). Molecular characterization of a peripheral receptor for cannabinoids. Nature *365*, 61–65. 10.1038/365061a0.

25. Devane, W.A., Dysarz, F.A., Johnson, M.R., Melvin, L.S., and Howlett, A.C. (1988).

Determination and characterization of a cannabinoid receptor in rat brain - PubMed. Mol Pharmacol *34*, 605–613.

26. Maccioni, P., Pes, D., Carai, M.A.M., Gessa, G.L., and Colombo, G. (2008). Suppression by the cannabinoid CB1 receptor antagonist, rimonabant, of the reinforcing and motivational properties of a chocolate-flavoured beverage in rats. Behav. Pharmacol. *19*, 197–209. 10.1097/FBP.0B013E3282FE8888.

27. Salamone, J.D., McLaughlin, P.J., Sink, K., Makriyannis, A., and Parker, L.A. (2007). Cannabinoid CB1 receptor inverse agonists and neutral antagonists: effects on food intake, food-reinforced behavior and food aversions. Physiol. Behav. *91*, 383–388. 10.1016/J.PHYSBEH.2007.04.013.

28. Thornton-Jones, Z.D., Vickers, S.P., and Clifton, P.G. (2005). The cannabinoid CB1 receptor antagonist SR141716A reduces appetitive and consummatory responses for food. Psychopharmacology (Berl). *179*, 452–460. 10.1007/S00213-004-2047-8.

29. McLaughlin, P.J., Winston, K., Swezey, L., Wisniecki, A., Aberman, J., Tardif, D.J., Betz, A.J., Ishiwari, K., Makriyannis, A., and Salamone, J.D. (2003). The cannabinoid CB1 antagonists SR 141716A and AM 251 suppress food intake and food-reinforced behavior in a variety of tasks in rats. Behav. Pharmacol. *14*, 583–588. 10.1097/00008877-200312000-00002.

30. Freedland, C.S., Poston, J.S., and Porrino, L.J. (2000). Effects of SR141716A, a central cannabinoid receptor antagonist, on food-maintained responding. Pharmacol. Biochem. Behav. *67*, 265–270. 10.1016/S0091-3057(00)00359-2.

31. Gallate, J.E., Saharov, T., Mallet, P.E., and McGregor, I.S. (1999). Increased motivation for beer in rats following administration of a cannabinoid CB1 receptor agonist. Eur. J.

803 Pharmacol. *370*, 233–240. 10.1016/S0014-2999(99)00170-3.
804 32. Gallate, J.E., and McGregor, I.S. (1999). The motivation for beer in rats: effects of
805 ritanserin, naloxone and SR 141716. Psychopharmacology (Berl). *142*, 302–308.
806 10.1007/S002130050893.
807 33. Guegan, T., Cutando, L., Ayuso, E., Santini, E., Fisone, G., Bosch, F., Martinez, A.,
808 Valjent, E., Maldonado, R., and Martin, M. (2013). Operant behavior to obtain palatable
809 food modifies neuronal plasticity in the brain reward circuit. Eur. Neuropsychopharmacol.
810 *23*, 146–159. 10.1016/J.EURONEURO.2012.04.004.
811 34. Barbano, M.F., Castañé, A., Martín-García, E., and Maldonado, R. (2009). Delta-9-
812 tetrahydrocannabinol enhances food reinforcement in a mouse operant conflict test.
813 Psychopharmacology (Berl). *205*, 475–487. 10.1007/s00213-009-1557-9.
814 35. Koch, J.E., and Matthews, S.M. (2001). Delta9-tetrahydrocannabinol stimulates palatable
815 food intake in Lewis rats: effects of peripheral and central administration. Nutr. Neurosci.
816 *4*, 179–187.
817 36. Brown, J.E., Kassouny, M., and Cross, J.K. (1977). Kinetic studies of food intake and
818 sucrose solution preference by rats treated with low doses of delta9-tetrahydrocannabinol.
819 Behav. Biol. *20*, 104–110.
820 37. Escartín-Pérez, R.E., Cendejas-Trejo, N.M., Cruz-Martínez, A.M., González-Hernández,
821 B., Mancilla-Díaz, J.M., and Florán-Garduño, B. (2009). Role of cannabinoid CB1
822 receptors on macronutrient selection and satiety in rats. Physiol. Behav. *96*, 646–650.
823 10.1016/J.PHYSBEH.2008.12.017.
824 38. Shinohara, Y., Inui, T., Yamamoto, T., and Shimura, T. (2009). Cannabinoid in the
825 nucleus accumbens enhances the intake of palatable solution. Neuroreport *20*, 1382–1385.

826 10.1097/WNR.0B013E3283318010.
827 39. Mathes, C.M., Ferrara, M., and Rowland, N.E. (2008). Cannabinoid-1 receptor antagonists
828 reduce caloric intake by decreasing palatable diet selection in a novel dessert protocol in
829 female rats. Am. J. Physiol. Regul. Integr. Comp. Physiol. *295*, R67.
830 10.1152/AJPREGU.00150.2008.
831 40. Gessa, G.L., Orrù, A., Lai, P., Maccioni, P., Lecca, R., Lobina, C., Carai, M.A.M., and
832 Colombo, G. (2006). Lack of tolerance to the suppressing effect of rimonabant on
833 chocolate intake in rats. Psychopharmacology (Berl). *185*, 248–254. 10.1007/S00213-006-
834 0327-1/FIGURES/4.
835 41. Arnone, M., Maruani, J., Chaperon, F., Thiébot, M.H., Poncelet, M., Soubrié, P., and Le
836 Fur, G. (1997). Selective inhibition of sucrose and ethanol intake by SR 141716, an
837 antagonist of central cannabinoid (CB1) receptors. Psychopharmacology (Berl). *132*, 104–
838 106.
839 42. Simiand, J., Keane, M., Keane, P.E., and Soubrié, P. (1998). SR 141716, a CB1
840 cannabinoid receptor antagonist, selectively reduces sweet food intake in marmoset.
841 Behav. Pharmacol. *9*, 179–181.
842 43. Castro, D.C., and Berridge, K.C. (2017). Opioid and orexin hedonic hotspots in rat
843 orbitofrontal cortex and insula. Proc. Natl. Acad. Sci. U. S. A. *114*, E9125–E9134.
844 10.1073/PNAS.1705753114/-/DCSUPPLEMENTAL.
845 44. Edwards, A., and Abizaid, A. (2016). Driving the need to feed: Insight into the
846 collaborative interaction between ghrelin and endocannabinoid systems in modulating
847 brain reward systems. Neurosci. Biobehav. Rev. *66*, 33–53.
848 10.1016/J.NEUBIOREV.2016.03.032.

45. Higgs, S., Williams, C.M., and Kirkham, T.C. (2003). Cannabinoid influences on palatability: microstructural analysis of sucrose drinking after Δ9-tetrahydrocannabinol, anandamide, 2-arachidonoyl glycerol and SR141716. Psychopharmacology (Berl). *165*, 370–377. 10.1007/s00213-002-1263-3.

46. Davis, J.D., and Smith, G.P. (1992). Analysis of the microstructure of the rhythmic tongue movements of rats ingesting maltose and sucrose solutions - PubMed. Behav Neurosci *106*, 217–228.

47. Grill, H.J., and Norgren, R. (1978). The taste reactivity test. I. Mimetic responses to gustatory stimuli in neurologically normal rats. Brain Res. *143*, 263–279. 10.1016/0006-8993(78)90568-1.

48. Jarrett, M.M., Limebeer, C.L., and Parker, L.A. (2005). Effect of Δ9-tetrahydrocannabinol on sucrose palatability as measured by the taste reactivity test. Physiol. Behav. *86*, 475–479. 10.1016/j.physbeh.2005.08.033.

49. Yoshida, R., Ohkuri, T., Jyotaki, M., Yasuo, T., Horio, N., Yasumatsu, K., Sanematsu, K., Shigemura, N., Yamamoto, T., Margolskee, R.F., et al. (2010). Endocannabinoids selectively enhance sweet taste. Proc. Natl. Acad. Sci. U. S. A. *107*, 935–939. 10.1073/pnas.0912048107.

50. Yoshida, R., Niki, M., Jyotaki, M., Sanematsu, K., Shigemura, N., and Ninomiya, Y. (2013). Modulation of sweet responses of taste receptor cells. Semin. Cell Dev. Biol. *24*, 226–231. 10.1016/J.SEMCDB.2012.08.004.

51. Soria-Gómez, E., Bellocchio, L., Reguero, L., Lepousez, G., Martin, C., Bendahmane, M., Ruehle, S., Remmers, F., Desprez, T., Matias, I., et al. (2014). The endocannabinoid system controls food intake via olfactory processes. Nat. Neurosci. *17*, 407–415.

10.1038/nn.3647.

52. Elphick, M.R. (2012). The evolution and comparative neurobiology of endocannabinoid signalling. Philos. Trans. R. Soc. B Biol. Sci. *367*, 3201–3215. 10.1098/rstb.2011.0394.

53. Raible, F., and Arendt, D. (2004). Metazoan Evolution: Some Animals Are More Equal than Others. Curr. Biol. *14*, R106–R108. 10.1016/j.cub.2004.01.015.

54. Estrada-Valencia, R., de Lima, M.E., Colonnello, A., Rangel-López, E., Saraiva, N.R., de Ávila, D.S., Aschner, M., and Santamaría, A. (2021). The Endocannabinoid System in Caenorhabditis elegans. 1–31. 10.1007/112_2021_64.

55. Oakes, M., Law, W.J., Clark, T., Bamber, B., and Komuniecki, R. (2017). Cannabinoids activate monoaminergic signaling to modulate key C. elegans behaviors. J. Neurosci. *37*, 2859–2869. 10.1523/JNEUROSCI.3151-16.2017.

56. Pastuhov, S.I., Matsumoto, K., and Hisamoto, N. (2016). Endocannabinoid signaling regulates regenerative axon navigation in *Caenorhabditis elegans* via the GPCRs NPR-19 and NPR-32. Genes to Cells *21*, 696–705. 10.1111/gtc.12377.

57. Oakes, M., Law, W.J., and Komuniecki, R. (2019). Cannabinoids stimulate the TRP channel-dependent release of both serotonin and dopamine to modulate behavior in C. elegans. J. Neurosci. *39*, 4142–4152. 10.1523/JNEUROSCI.2371-18.2019.

58. Lehtonen, M., Reisner, K., Auriola, S., Wong, G., and Callaway, J.C. (2008). Mass-Spectrometric Identification of Anandamide and 2-Arachidonoylglycerol in Nematodes. Chem. Biodivers. *5*, 2431–2441. 10.1002/cbdv.200890208.

59. Lehtonen, M., Storvik, M., Malinen, H., Hyytiä, P., Lakso, M., Auriola, S., Wong, G., and Callaway, J.C. (2011). Determination of endocannabinoids in nematodes and human brain tissue by liquid chromatography electrospray ionization tandem mass spectrometry. J.

Chromatogr. B *879*, 677–694. 10.1016/J.JCHROMB.2011.02.004.

60. Sugiura, T., Kondo, S., Sukagawa, A., Nakane, S., Shinoda, A., Itoh, K., Yamashita, A., and Waku, K. (1995). 2-Arachidonoylgylcerol: A Possible Endogenous Cannabinoid Receptor Ligand in Brain. Biochem. Biophys. Res. Commun. *215*, 89–97. 10.1006/BBRC.1995.2437.

61. Harrison, N., Lone, M.A., Kaul, T.K., Reis Rodrigues, P., Ogungbe, I.V., and Gill, M.S. (2014). Characterization of N-Acyl Phosphatidylethanolamine-Specific Phospholipase-D Isoforms in the Nematode Caenorhabditis elegans. PLoS One *9*, e113007. 10.1371/journal.pone.0113007.

62. Pastuhov, S.I., Fujiki, K., Nix, P., Kanao, S., Bastiani, M., Matsumoto, K., and Hisamoto, N. (2012). Endocannabinoid-Goα signalling inhibits axon regeneration in Caenorhabditis elegans by antagonizing Gqα-PKC-JNK signalling. Nat. Commun. *3*, 1136. 10.1038/ncomms2136.

63. Lucanic, M., Held, J.M., Vantipalli, M.C., Klang, I.M., Graham, J.B., Gibson, B.W., Lithgow, G.J., and Gill, M.S. (2011). N-acylethanolamine signalling mediates the effect of diet on lifespan in Caenorhabditis elegans. Nature *473*, 226–229. 10.1038/nature10007.

64. Reis-Rodrigues, P., Kaul, T.K., Ho, J.-H., Lucanic, M., Burkewitz, K., Mair, W.B., Held, J.M., Bohn, L.M., and Gill, M.S. (2016). Synthetic Ligands of Cannabinoid Receptors Affect Dauer Formation in the Nematode Caenorhabditis elegans. G3 (Bethesda). *6*, 1695–1705. 10.1534/g3.116.026997.

65. Frézal, L., and Félix, M.A. (2015). The Natural History of Model Organisms: C. elegans outside the Petri dish. Elife *2015*. 10.7554/ELIFE.05849.001.

66. Bargmann, C.I., and Horvitz, H.R. (1991). Chemosensory neurons with overlapping

functions direct chemotaxis to multiple chemicals in C. elegans. Neuron *7*, 729–742. 10.1016/0896-6273(91)90276-6.

67. Bargmann, C.I., Hartwieg, E., and Horvitz, H.R. (1993). Odorant-selective genes and neurons mediate olfaction in C. elegans. Cell *74*, 515–527. 10.1016/0092-8674(93)80053-H.

68. Avery, L., and Shtonda, B.B. (2003). Food transport in the C. elegans pharynx. J. Exp. Biol. 10.1242/jeb.00433.

69. Shtonda, B.B. (2006). Dietary choice behavior in Caenorhabditis elegans. J. Exp. Biol. 10.1242/jeb.01955.

70. Raizen, D.M., and Avery, L. (1994). Electrical Activity and Behavior in the Pharynx of Caenorhabditis elegans. Neuron *12*, 483–495.

71. Lockery, S.R., Hulme, S.E., Roberts, W.M., Robinson, K.J., Laromaine, A., Lindsay, T.H., Whitesides, G.M., and Weeks, J.C. (2012). A microfluidic device for whole-animal drug screening using electrophysiological measures in the nematode C. elegans. Lab Chip *12*, 2211–2220. 10.1039/c2lc00001f.

72. Oakes, M.D., Law, W.J., Clark, T., Bamber, B.A., and Komuniecki, R. (2017). Cannabinoids Activate Monoaminergic Signaling to Modulate KeyC. elegansBehaviors. J. Neurosci. *37*, 2859–2869. 10.1523/JNEUROSCI.3151-16.2017.

73. Hart, A.C. (2006). Behavior. In WormBook (The C. elegans Research Community). 10.1895/WORMBOOK.1.87.1.

74. Zaslaver, A., Liani, I., Shtangel, O., Ginzburg, S., Yee, L., and Sternberg, P.W. (2015). Hierarchical sparse coding in the sensory system of Caenorhabditis elegans. Proc. Natl. Acad. Sci. U. S. A. *112*, 1185–1189. 10.1073/pnas.1423656112.

75. Leinwand, S.G., Yang, C.J., Bazopoulou, D., Chronis, N., Srinivasan, J., and Chalasani, S.H. (2015). Circuit mechanisms encoding odors and driving aging-associated behavioral declines in Caenorhabditis elegans. Elife *4*, 1–26. 10.7554/eLife.10181.

76. Koga, M., and Ohshima, Y. (2004). The C . elegans ceh-36 Gene Encodes a Putative Homemodomain Transcription Factor Involved in Chemosensory Functions of ASE and AWC Neurons. J. Mol. Biol. *336*, 579–587. 10.1016/j.jmb.2003.12.037.

77. Lanjuin, A., Vanhoven, M.K., Bargmann, C.I., Thompson, J.K., and Sengupta, P. (2003). Otx / otd Homeobox Genes Specify Distinct Sensory Neuron Identities in C . elegans. Dev. Cell *5*, 621–633.

78. Calhoun, A.J., Tong, A., Pokala, N., Fitzpatrick, J.A.J., Sharpee, T.O., and Chalasani, S.H. (2015). Neural mechanisms for evaluating environmental variability in caenorhabditis elegans. Neuron *86*, 428–441. 10.1016/j.neuron.2015.03.026.

79. Chalasani, S.H., Chronis, N., Tsunozaki, M., Gray, J.M., Ramot, D., Goodman, M.B., and Bargmann, C.I. (2007). Dissecting a circuit for olfactory behaviour in Caenorhabditis elegans. Nature *450*, 63–70. 10.1038/nature06292.

80. Pierce-Shimomura, J.T., Morse, T.M., and Lockery, S.R. (1999). The Fundamental Role of Pirouettes in Caenorhabditis elegans Chemotaxis. J. Neurosci. *19*, 9557–9569. 10.1523/JNEUROSCI.19-21-09557.1999.

81. Serrano-Saiz, E., Poole, R.J., Felton, T., Zhang, F., De La Cruz, E.D., and Hobert, O. (2013). Modular Control of Glutamatergic Neuronal Identity in C. elegans by Distinct Homeodomain Proteins. Cell *155*, 659–673. 10.1016/J.CELL.2013.09.052.

82. Pereira, L., Kratsios, P., Serrano-Saiz, E., Sheftel, H., Mayo, A.E., Hall, D.H., White, J.G., LeBoeuf, B., Garcia, L.R., Alon, U., et al. (2015). A cellular and regulatory map of the

964 cholinergic nervous system of C. elegans. Elife *4*, e12432. 10.7554/eLife.12432.
965 83. Hammarlund, M., Hobert, O., Miller, D.M., and Sestan, N. (2018). The CeNGEN Project:
966 The Complete Gene Expression Map of an Entire Nervous System. Neuron *99*, 430–433.
967 10.1016/j.neuron.2018.07.042.
968 84. Good, C.H. (2007). Endocannabinoid-dependent regulation of feedforward inhibition in
969 cerebellar purkinje cells. J. Neurosci. *27*, 1–3. 10.1523/JNEUROSCI.4842-06.2007.
970 85. Wormatlas https://www.wormatlas.org.
971 86. Richmond, J.E., Davis, W.S., and Jorgensen, E.M. (1999). UNC-13 is required for
972 synaptic vesicle fusion in C. elegans. Nat. Neurosci. *2*, 959–964. 10.1038/14755.
973 87. Probert, L., De Mey, J., and Polak, J.M. (1983). Ultrastructural localization of four
974 different neuropeptides within separate populations of p-type nerves in the guinea pig
975 colon. Gastroenterology *85*, 1094–1104. 10.1016/S0016-5085(83)80077-8.
976 88. Devine, C.E., and Simpson, F.O. (1968). Localization of tritiated norepinephrine in
977 vascular sympathetic axons of the rat intestine and mesentery by electron microscope
978 radioautography. J. Cell Biol. *38*, 184–192. 10.1083/JCB.38.1.184.
979 89. Speese, S., Petrie, M., Schuske, K., Ailion, M., Ann, K., Iwasaki, K., Jorgensen, E.M., and
980 Martin, T.F.J. (2007). UNC-31 (CAPS) Is Required for Dense-Core Vesicle But Not
981 Synaptic Vesicle Exocytosis in Caenorhabditis elegans. J. Neurosci. *27*, 6150–6162.
982 10.1523/JNEUROSCI.1466-07.2007.
983 90. Sowa, J.N., Mutlu, A.S., Xia, F., and Wang, M.C. (2015). Olfaction Modulates
984 Reproductive Plasticity through Neuroendocrine Signaling in Caenorhabditis elegans.
985 Curr. Biol. *25*, 2284–2289. 10.1016/j.cub.2015.07.023.
986 91. So, S., Miyahara, K., and Ohshima, Y. (2011). Control of body size in C. elegans

dependent on food and insulin/IGF-1 signal. Genes to Cells *16*, 639–651. 10.1111/j.1365-2443.2011.01514.x.

92. Avery, L., and Horvitzt, H.R. (1989). Pharyngeal pumping continues after laser killing of the pharyngeal nervous system of C. elegans. Neuron *3*, 473–485. 10.1016/0896-6273(89)90206-7.

93. Raizen, D.M., Lee, R.Y., and Avery, L. (1995). Interacting genes required for pharyngeal excitation by motor neuron MC in Caenorhabditis elegans. Genetics *141*, 1365–1382. 10.1093/GENETICS/141.4.1365.

94. Avery, L. (1993). Motor neuron M3 controls pharyngeal muscle relaxation timing in Caenorhabditis elegans. J. Exp. Biol. *175*, 283–297. 10.1242/JEB.175.1.283.

95. De Petrocellis, L., Melck, D., Bisogno, T., Milone, A., and Di Marzo, V. (1999). Finding of the endocannabinoid signalling system in Hydra, a very primitive organism: possible role in the feeding response. Neuroscience *92*, 377–387. 10.1016/S0306-4522(98)00749-0.

96. Park, S.H., Staples, S.K., Gostin, E.L., Smith, J.P., Vigil, J.J., Seifried, D., Kinney, C., Pauli, C.S., and Heuvel, B.D.V. (2019). Contrasting Roles of Cannabidiol as an Insecticide and Rescuing Agent for Ethanol-induced Death in the Tobacco Hornworm Manduca sexta. Sci. Rep. *9*. 10.1038/S41598-019-47017-7.

97. He, J., Tan, A.M.X., Ng, S.Y., Rui, M., and Yu, F. (2021). Cannabinoids modulate food preference and consumption in Drosophila melanogaster. Sci. Rep. *11*, 1–13. 10.1038/s41598-021-84180-2.

98. DiPatrizio, N. V., and Simansky, K.J. (2008). Activating parabrachial cannabinoid CB1 receptors selectively stimulates feeding of palatable foods in rats. J. Neurosci. *28*, 9702–

9709. 10.1523/JNEUROSCI.1171-08.2008.

99. Williams, C.M., Rogers, P.J., and Kirkham, T.C. (1998). Hyperphagia in pre-fed rats following oral δ9-THC. Physiol. Behav. *65*, 343–346. 10.1016/S0031-9384(98)00170-X.

100. Salamone, J.D., Cousins, M.S., and Bucher, S. (1994). Anhedonia or anergia? Effects of haloperidol and nucleus accumbens dopamine depletion on instrumental response selection in a T-maze cost/benefit procedure. Behav. Brain Res. *65*, 221–229. 10.1016/0166-4328(94)90108-2.

101. Kocabas, A., Shen, C.H., Guo, Z. V., and Ramanathan, S. (2012). Controlling interneuron activity in Caenorhabditis elegans to evoke chemotactic behaviour. Nature *490*, 273–277. 10.1038/nature11431.

102. Heinbockel, T., and Straiker, A. (2021). Cannabinoids Regulate Sensory Processing in Early Olfactory and Visual Neural Circuits. Front. Neural Circuits *15*. 10.3389/FNCIR.2021.662349.

103. Nogi, Y., Ahasan, M.M., Murata, Y., Taniguchi, M., Sha, M.F.R., Ijichi, C., and Yamaguchi, M. (2020). Expression of feeding-related neuromodulatory signalling molecules in the mouse central olfactory system. Sci. Rep. *10*. 10.1038/S41598-020-57605-7.

104. Fraenkel, G.S., and Gunn, D.L. (1961). The orientation of animals: Kineses, taxes and compass reactions. - PsycNET (Dover).

105. Gordus, A., Pokala, N., Levy, S., Flavell, S.W., and Bargmann, C.I. (2015). Feedback from network states generates variability in a probabilistic olfactory circuit. Cell *161*, 215–227. 10.1016/j.cell.2015.02.018.

106. Gray, J.M., Hill, J.J., and Bargmann, C.I. (2005). A dual mechanosensory and

chemosensory neuron in Caenorhabditis elegans. PNAS *90*, 2227–2231. 10.1073/pnas.90.6.2227.

107. Chalasani, S.H., Kato, S., Albrecht, D.R., Nakagawa, T., Abbott, L.F., and Bargmann, C.I. (2010). Neuropeptide feedback modifies odor-evoked dynamics in Caenorhabditis elegans olfactory neurons. Nat. Neurosci. *13*, 615–621. 10.1038/nn.2526.

108. Leinwand, S.G., and Chalasani, S.H. (2013). Neuropeptide signaling remodels chemosensory circuit composition in Caenorhabditis elegans. Nat. Neurosci. *16*, 1461–1467. 10.1038/nn.3511.

109. Parsons, L.H., and Hurd, Y.L. (2015). Endocannabinoid signalling in reward and addiction. Nat. Rev. Neurosci. *16*, 579–594. 10.1038/NRN4004.

110. WormAtlas https://www.wormatlas.org/.

111. Brenner, S. (1974). The genetics of Caenorhabditis elegans. Genetics *77*, 71–94. 10.1093/genetics/77.1.71.

112. Rand, J.B., and Johnson, C.D. (1995). Genetic pharmacology: interactions between drugs and gene products in Caenorhabditis elegans. Methods Cell Biol. *48*, 187–204. 10.1016/S0091-679X(08)61388-6.

113. Sandhu, A., Badal, D., Sheokand, R., Tyagi, S., and Singh, V. (2021). Specific collagens maintain the cuticle permeability barrier in Caenorhabditis elegans. Genetics *217*. 10.1093/GENETICS/IYAA047.

114. Mathew, M.D., Mathew, N.D., and Ebert, P.R. (2012). WormScan: A technique for high-throughput phenotypic analysis of Caenorhabditis elegans. PLoS One *7*, e33483. 10.1371/journal.pone.0033483.

115. Stroustrup, N., Ulmschneider, B.E., Nash, Z.M., López-Moyado, I.F., Apfeld, J., and

Fontana, W. (2013). The caenorhabditis elegans lifespan machine. Nat. Methods *10*, 665–670. 10.1038/nmeth.2475.

116. Collins, T.J. (2007). ImageJ for microscopy. Biotechniques *43*, S25–S30. 10.2144/000112517.

117. Keppel, G., and Zedeck, S. (1989). Data analysis for research designs : analysis-of-variance and multiple regression/correlation approaches. 594.

KEY RESOURCES TABLE

REAGENT or RESOURCE	SOURCE	IDENTIFIER
Bacterial strains		
OP50	*C. elegans* Genetic Center (CGC)	RRID:WB-STRAIN:WBStrain00041969
DA1877	CGC	RRID:WB-STRAIN:WBStrain00040995
DA1885	CGC	RRID:WB-STRAIN:WBStrain00040997
DA837	CGC	RRID:WB-STRAIN:WBStrain00040994
HB101	CGC	RRID:WB-STRAIN:WBStrain00041075
DA1881 (S13)	Raizen lab DOI: 10.1242/jeb.00433	
C. elegans strains (genotype)		
N2, Bristol Wild type	CGC	RRID:WB-STRAIN:WBStrain00000001
FK311 *ceh-36*(ks86)	CGC	RRID:WB-STRAIN:WBStrain00007515
RB1668 *npr-19*(ok2068)	CGC	RRID:WB-STRAIN:WBStrain00032361
C02H7.2(tm2574) *npr-19*(tm2574)	National Bioresource Project for the Experimental Animal "Nematode C. elegans"	
XL324 ntIS1701[*npr-19*::CNR1::gfp-*npr-19*(1.1);*unc-122*::RFP]	This manuscript	
XL325 ntIS1702[*npr*-19::*npr-19*::gfp-*npr-19*(1.1)]	This manuscript	
XL322 ntIS1703[*str-2*::GCaMP6::wCherry;*unc-122*::dsRed]	This manuscript	
XL327 *unc-13*(e51);ntIs1703[*str-2*::GCaMP6::wCherry;*unc-122*::dsRed]	This manuscript	

XL326 *unc-31*(e928);ntIs1703[*str-2*::GCaMP6::wCherry;*unc-122*::dsRed]	This manuscript	
XL346 *npr-19*(ok2068);ntIs1912[*str-2*::GCaMP6::wCherry;*unc-122*::dsRed]	This manuscript	
XL348 *npr-19*(ok2068);ntIs2301[npr-19::npr-19,str-2::GCamp6+wormcherry,unc-122::dsred]	This manuscript	
XL334 otIs544[cho-1::SL2::mCherry::H2B+pha-1(+)];ntIS19114[npr-19::GFP1.1;unc-122::dsred]	This manuscript	
XL335 ntIS19114[npr-19::GFP1.1;unc-122::dsred];otIs518[eat-4::SL2::mCherry::H2B+pha-1(+)]	This manuscript	
Software		
MATLAB	MathWorks https://www.mathworks.com	R2022a (9.12)
Igor Pro	Wavemetrics https://www.wavemetrics.com/	Version 9.01
R studio	R Core Team https://www.r-project.org/	Version 2022.12.0+353

Figure 1

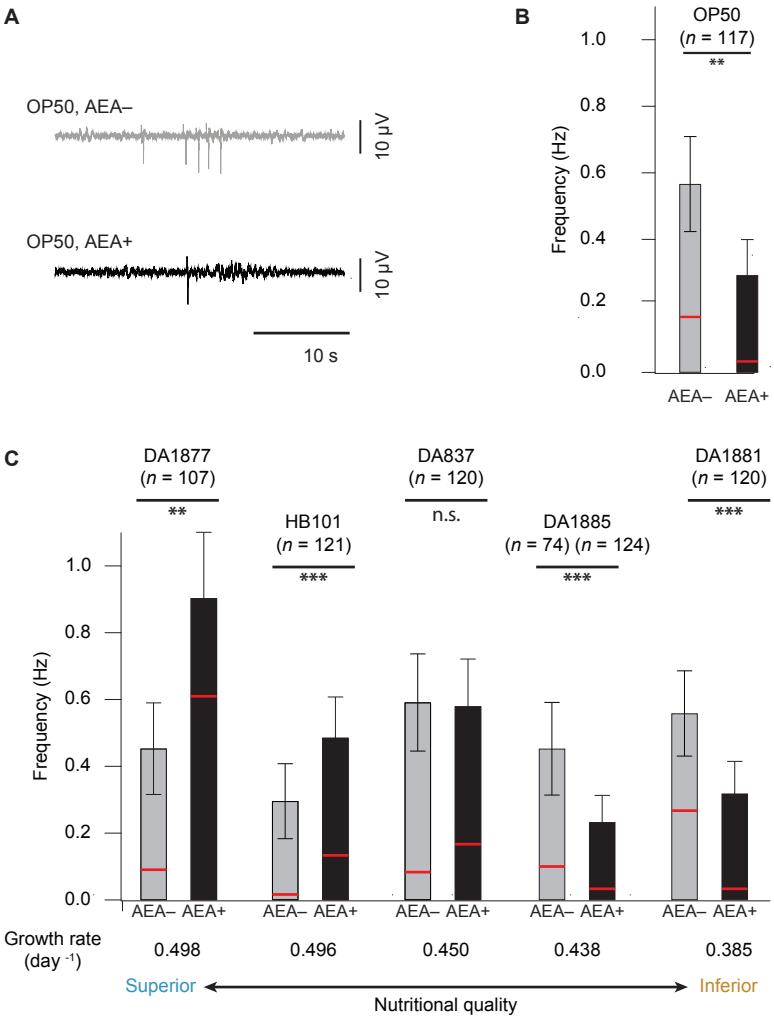
A
OP50, AEA–
10 µV
OP50, AEA+
10 µV
10 s
B
OP50
(n = 117)
**
Frequency (Hz)
1.0
0.8
0.6
0.4
0.2
0.0
AEA– AEA+
C
DA1877
(n = 107)
**
HB101
(n = 121)
***
DA837
(n = 120)
n.s.
DA1885
(n = 74) (n = 124)
***
DA1881
(n = 120)
***
Frequency (Hz)
1.0
0.8
0.6
0.4
0.2
0.0
AEA– AEA+ AEA– AEA+ AEA– AEA+ AEA– AEA+ AEA– AEA+
Growth rate
(day -1)
0.498
0.496
0.450
0.438
0.385
Superior
Inferior
Nutritional quality

Figure 2

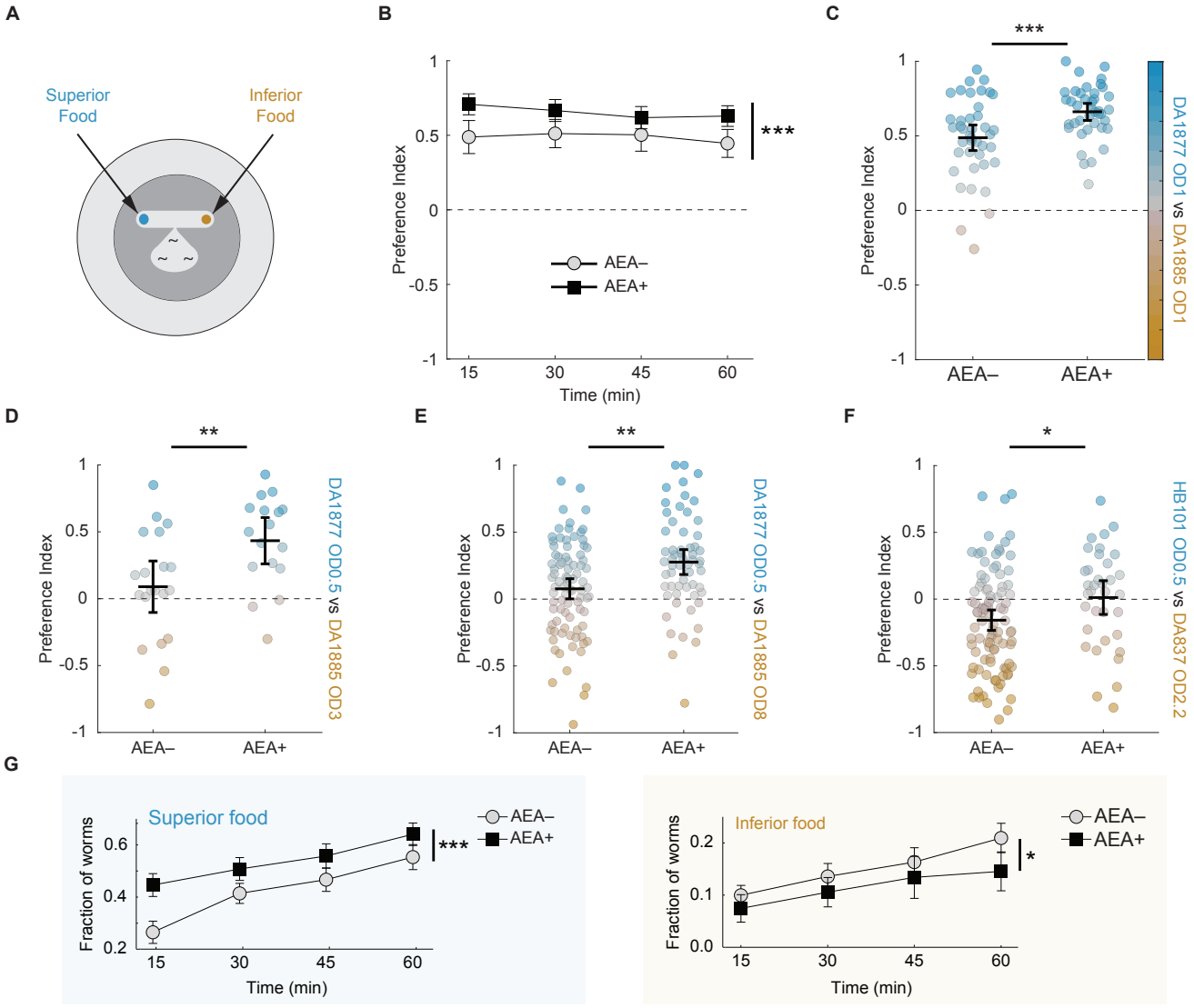
A
Superior Food
Inferior Food
B
Preference Index
Time (min)
AEA–
AEA+
***
C
***
Preference Index
AEA–
AEA+
DA1877 OD1 vs DA1885 OD1
D
**
Preference Index
AEA–
AEA+
DA1877 OD0.5 vs DA1885 OD3
E
**
Preference Index
AEA–
AEA+
DA1877 OD0.5 vs DA1885 OD8
F
*
Preference Index
AEA–
AEA+
HB101 OD0.5 vs DA837 OD2.2
G
Superior food
Fraction of worms
Time (min)
AEA–
AEA+
***
Inferior food
Fraction of worms
Time (min)
AEA–
AEA+
*

Figure 3

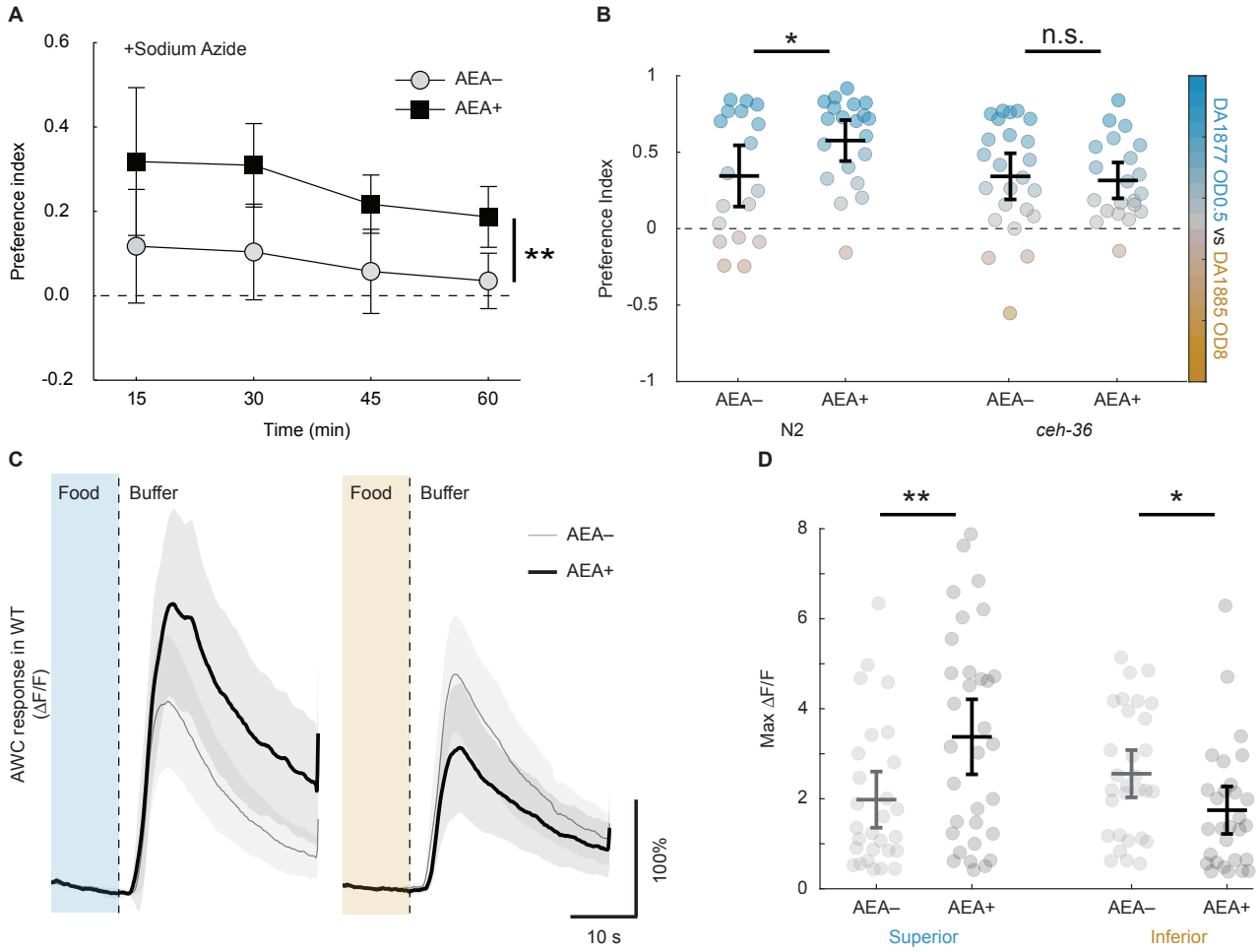
A
+Sodium Azide
AEA–
AEA+
Preference index
Time (min)
**
B
*
n.s.
Preference Index
DA1877 OD0.5 vs DA1885 OD8
AEA–
AEA+
N2
ceh-36
C
Food
Buffer
AWC response in WT (ΔF/F)
100%
10 s
D
Max ΔF/F
Superior
Inferior

Figure 4

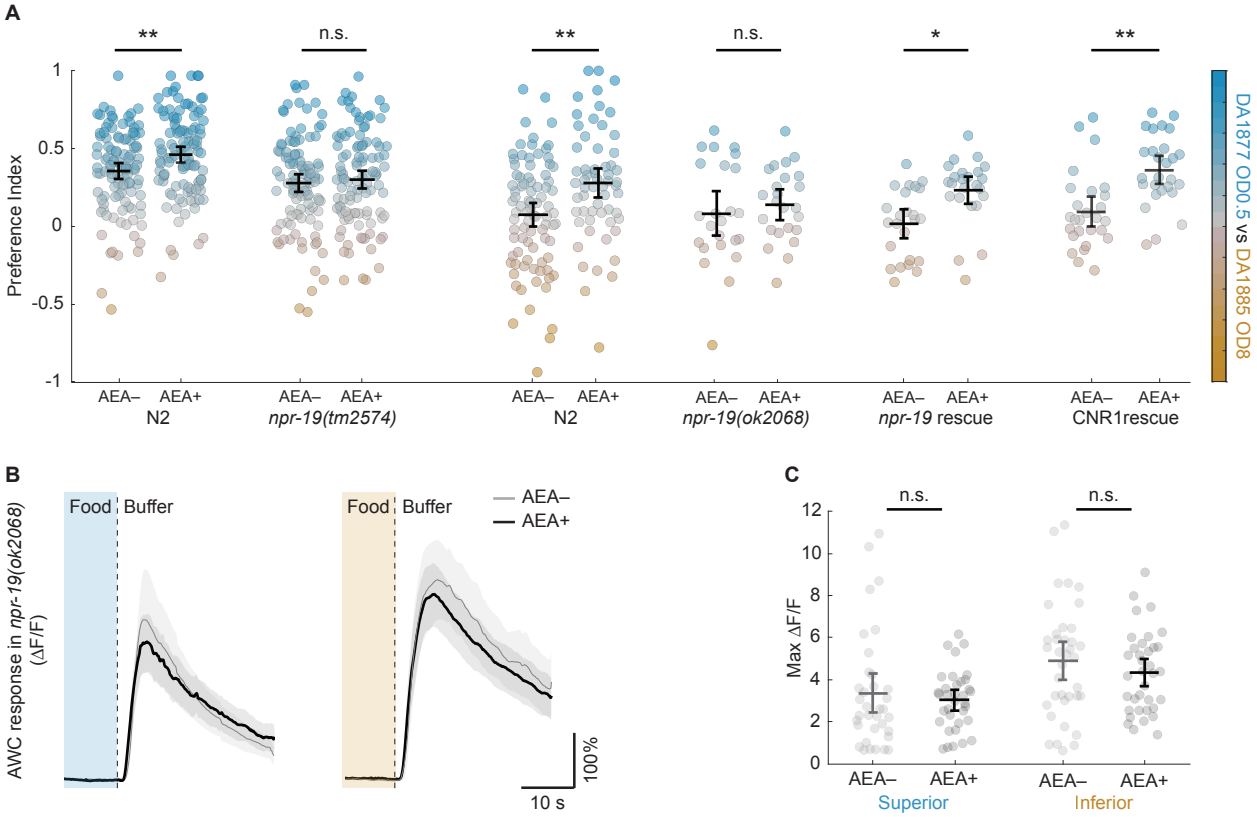
A
**
n.s.
**
n.s.
*
**
Preference Index
1
0.5
0
-0.5
-1
AEA–
AEA+
N2
npr-19(tm2574)
N2
npr-19(ok2068)
npr-19 rescue
CNR1rescue
DA1877 OD0.5 vs DA1885 OD8
B
Food
Buffer
AEA–
AEA+
AWC response in npr-19(ok2068) (ΔF/F)
100%
10 s
C
n.s.
n.s.
Max ΔF/F
12
10
8
6
4
2
0
Superior
Inferior

Figure 5

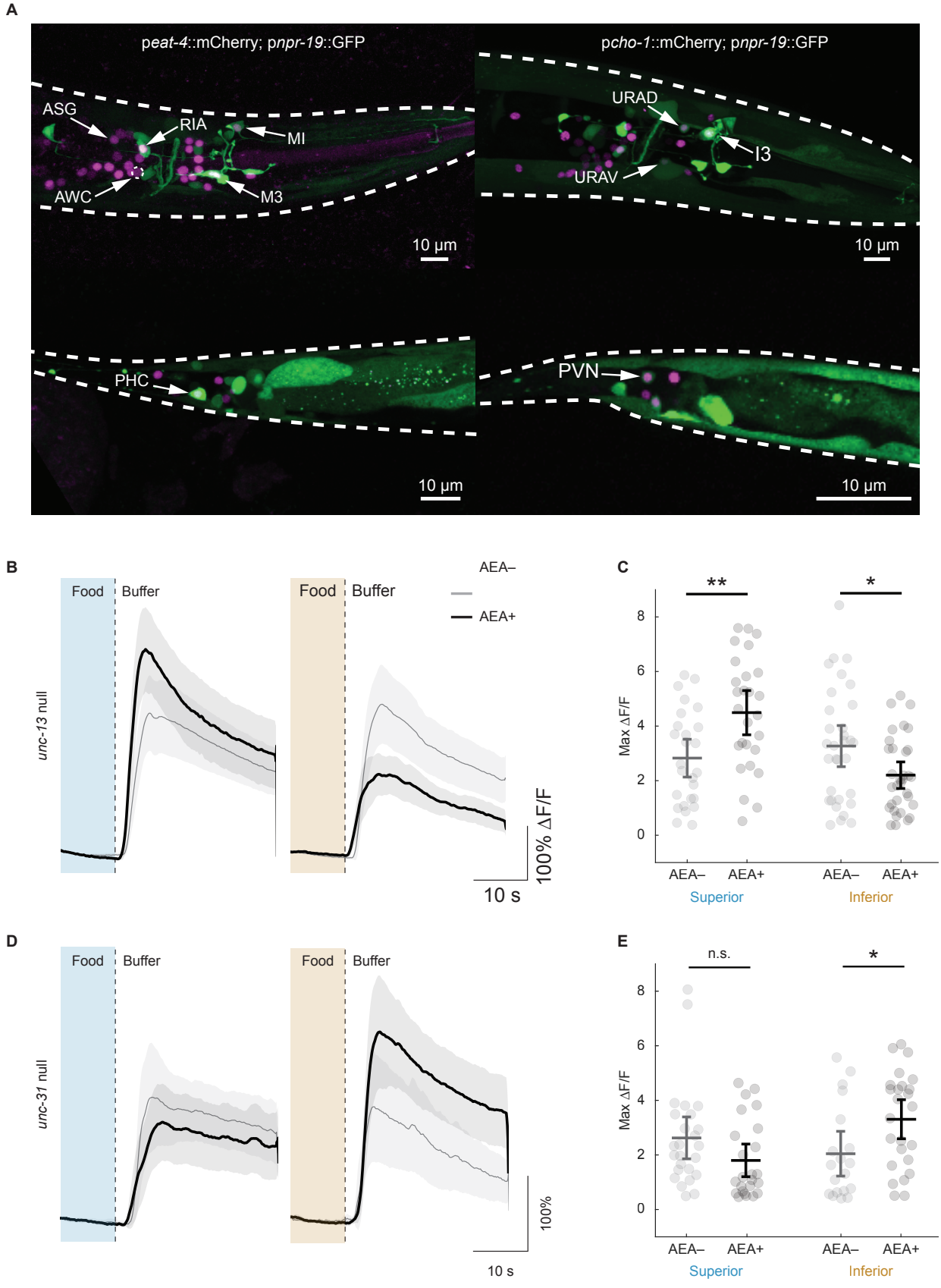
A
peat-4::mCherry; pnpr-19::GFP
ASG
RIA
MI
AWC
M3
10 µm
pcho-1::mCherry; pnpr-19::GFP
URAD
I3
URAV
10 µm
PHC
10 µm
PVN
10 µm
B
Food
Buffer
Food
Buffer
AEA–
AEA+
unc-13 null
100% ΔF/F
10 s
C
**
*
Max ΔF/F
0
2
4
6
8
AEA–
AEA+
AEA–
AEA+
Superior
Inferior
D
Food
Buffer
Food
Buffer
unc-31 null
100%
10 s
E
n.s.
*
Max ΔF/F
0
2
4
6
8
AEA–
AEA+
AEA–
AEA+
Superior
Inferior

Figure 6

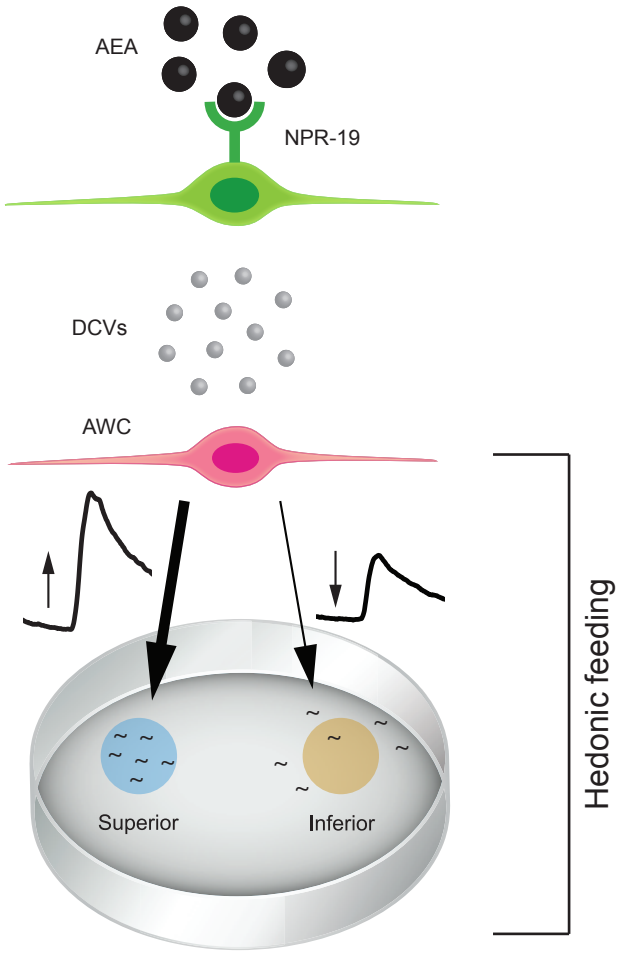

Table 1

Function	Identity of *npr-19*::GFP+ neurons	*eat-4*::mCherry expression	*cho-1*::mCherry expression	Cell body position and	CenGen *npr-19* expression	Transmitters	*unc-31 expression*
Pharyngeal	M3 L/R	*				Glu, FLP-18, NLP-3	
	MI	*			*	Glu	*
	MC L/R			*	*	Ach, FLP-21	*
	I2 L/R	*				Glu, NLP-3, NLP-8	*
	I4			*	*	NLP-3, NLP-13	*
	M1			*	*	Ach, NLP-3	*
Sensory	PHC L/R	*			*	Glu	
	URX L/R		*		*	Ach, FLP-8, FLP-10, FLP-11, FLP-19	*
	ASG L/R	*			*	Glu, 5HT, FLP-6, FLP-13, FLP-22, INS-1	*
	AWA L/R			*	*	INS-1	*
Interneuron	RIA L/R	*				Glu	*
	RIM L/R	*			*	Glu, Tyr	
	LUA L/R	*			*	Glu, NLP-13, PDF-1	
Motor	URA D/V L/R		*		*	ACh	*
	PDA		*		*	ACh	*

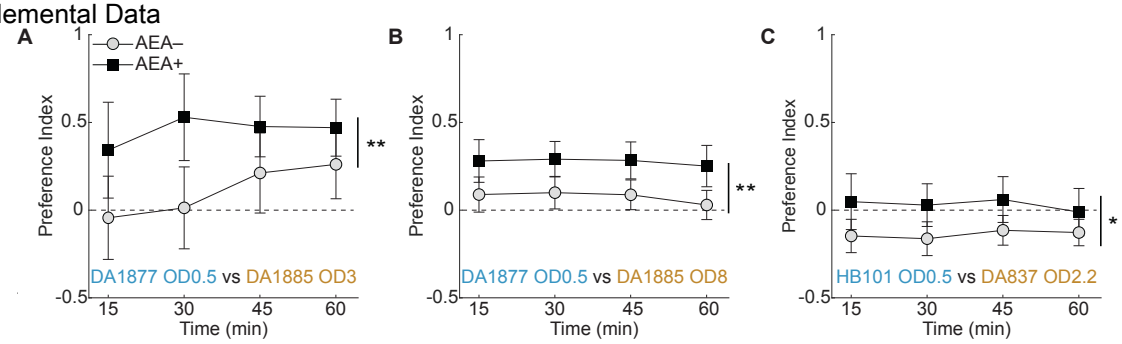

Figure S1. Effect of baseline preference and bacteria identity on preference time course, Related to Figure 2.

Mean preference index (*I*) versus time for AEA-exposed animals (AEA+) and unexposed controls (AEA–) corresponding to text figures 2D (**A**), 2E (**B**) and 2F (**C**). $I > 0$ is preference for superior food, $I < 0$ is preference for inferior food, and $I = 0$ is indifference (dashed line). For statistics, see Table S2. Symbols: *, $p < 0.05$; **, $p < 0.01$; n.s., not significant. Error bars, 95% confidence intervals.

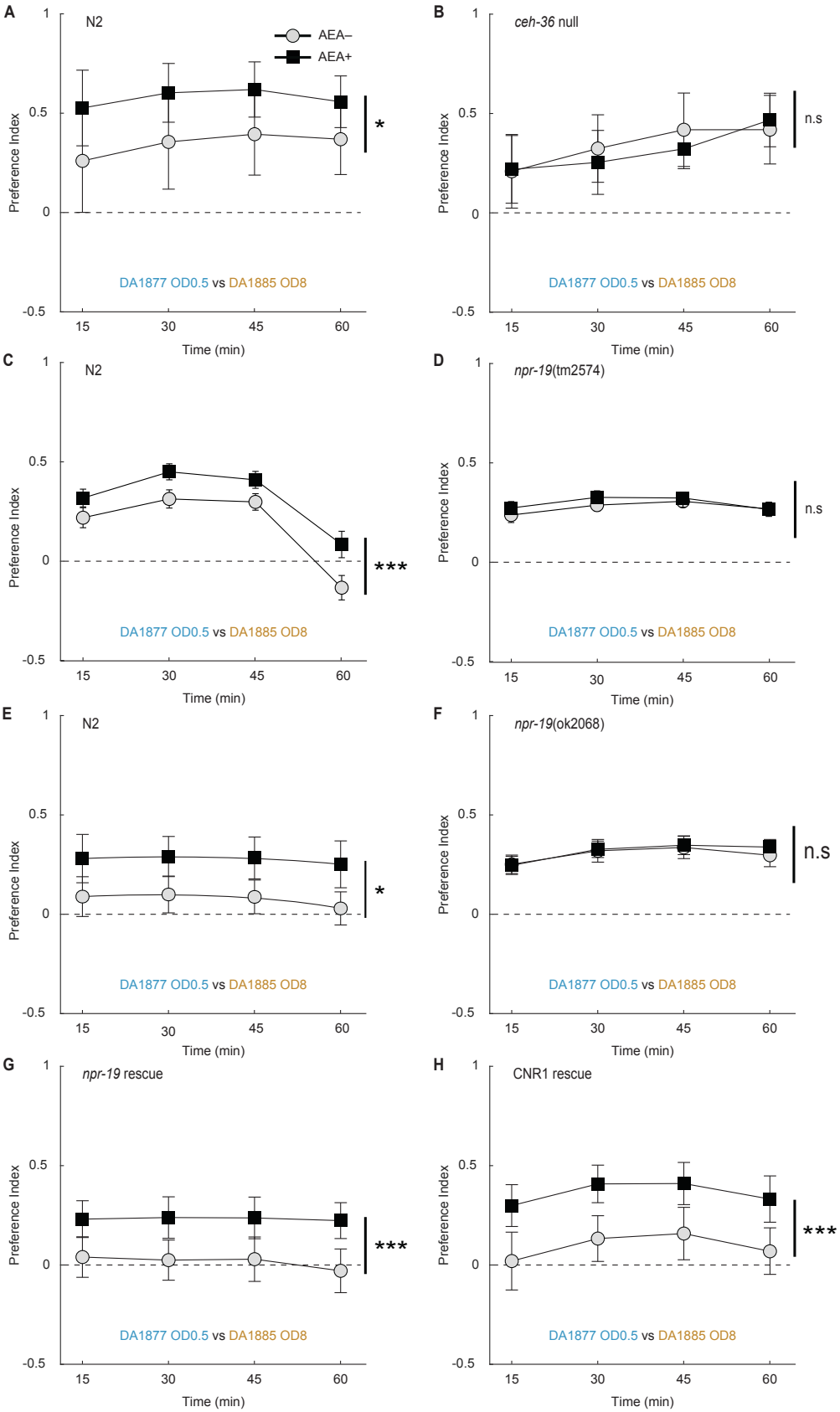

Figure S2. Effect of genetic background on preference time course, Related to Figures 3 and 4.

Mean preference index (*I*) versus time for AEA-exposed animals (AEA+) and unexposed controls (AEA–) corresponding to text figures 3B, *ceh-36* and contemporaneous N2 controls (**A, B**), Figure 4A, *npr-19*(tm2574) and contemporaneous N2 controls (**C,D**), Figure 4A, *npr-19*(ok2068) (**F**), Figure 4A, *npr-19* rescue (**G**), Figure 4A, CNR1 rescue (**H**) and contemporaneous N2 controls (E). $I > 0$ is preference for superior food, $I < 0$ is preference for inferior food, and $I = 0$ is indifference (dashed line). For statistics, see Tables S3, S4. Symbols: *, $p < 0.05$; ***, $p < 0.001$; n.s., not significant. Error bars, 95% confidence intervals.

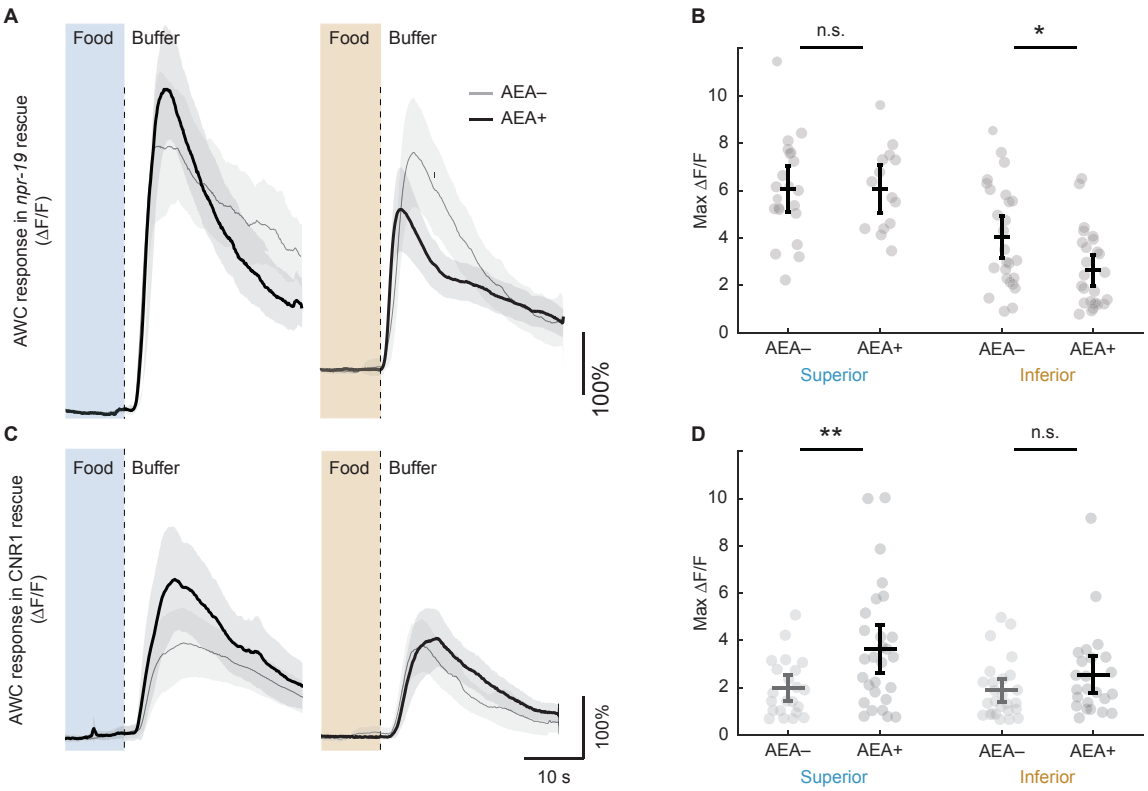

Figure S3. Partial rescue of AEA sensitivity in AWC neurons by *npr-19* and CNR1, Related to Figure 4.

A. Effect of AEA on amplitude of AWC calcium transients in response to the removal of superior or inferior food in a strain in which *npr-19* is overexpressed under the control of the *npr-19* promoter. **B**. Summary of the data in A, showing mean peak $\Delta F/F$. C, D, Same as A, B but for a strain in which CNR1 was overexpressed under control of the *npr-19* promoter. For statistics in B, C, see Table S6. Symbols: **, $p < 0.01$. Error bars and shading, 95% confidence intervals.

Line	Figure	Condition	Test	Number of replicates	Statistic	p-value	Significance	AEA– avg +/-CI	AEA+ avg +/-CI	Effect size
1	Figure 1B	OP50 OD 0.8	Mann-Whitney	n=117 (AEA–) n=117 (AEA+)	U= 5191	0.001	**	0.57 ± 0.14	0.29 ± 0.11	-0.30
2	Figure 1C	DA1877 OD 0.8	Mann-Whitney	n=107 (AEA–) n=107 (AEA+)	U= 7271.5	0.001	**	0.45 ± 0.14	0.90 ± 0.20	0.33
3	Figure 1C	HB101 OD 0.8	Mann-Whitney	*n=121 (AEA–)* *n=121 (AEA+)*	U= 9295	0.000	***	0.30 ± 0.11	0.49 ± 0.12	0.34
4	Figure 1C	DA837 OD 0.8	Mann-Whitney	*n=120 (AEA–)* *n=120 (AEA+)*	U= 7492	0.584		0.59 ± 0.15	0.58 ± 0.14	
5	Figure 1C	DA1885 OD 0.8	Mann-Whitney	*n=74 (AEA–)* *n=124 (AEA+)*	U= 3196.5.	0.000	***	0.45 ± 0.14	0.23 ± 0.08	-0.42
6	Figure 1C	B. cereus OD 0.8	Mann-Whitney	*n=120 (AEA–)* *n=120 (AEA+)*	U= 5275.5	0.000	***	0.56 ± 0.13	0.32 ± 0.10	-0.33

Table S1. Statistics for Figure 1.

Frequency of pumps in EPG recordings ± AEA. Unit of replication: individual worm. Experimental conditions are described in column 3. Stars in the Significance column indicate significance levels: *, $p < 0.05$; **, $p < 0.01$; ***, $p < 0.001$. Effect sizes were computed as described in Materials and Methods and 95% confidence intervals were used as a dispersion measure.

Line	Figure	Condition	Test	Number of replicates	Statistic	p-value	Significance	AEA– avg +/-CI	AEA+ avg +/-CI	Effect size
1	Figure 2B, 2C	DA1877 OD 1 DA1885 OD 1	Two-factor ANOVA, repeated measures	*n=41 (AEA–)* *n=40 (AEA+)*						
2			Main effect of AEA		F(1,79)= 11.00	0.001	***	0.49 ± 0.09	0.66 ± 0.06	0.12
3			Main effect of time		F(3,79)= 1.73	0.162				
4			Interaction, AEA × time		F(3,237)= 1.10	0.351				
5	Figure 2D Figure S1A	DA1877 OD 0.5 DA1885 OD 3	Two-factor ANOVA, repeated measures	*n=20 (AEA–)* *n=17 (AEA+)*						
6			Main effect of AEA		F(1,35)= 7.58	0.009	**	0.09 ± 0.19	0.43 ± 0.17	0.18
7			Main effect of time		F(3,35)= 4.10	0.009	**			
8			Interaction, AEA × time		F(3,105)= 2.00	0.118				
9	Figure 2E Figure S1B	DA1877 OD 0.5 DA1885 OD 8	Two-factor ANOVA, repeated measures	*n=86 (AEA–)* *n=59 (AEA+)*						
10			Main effect of AEA		F(1,143)= 11.16	0.001	**	0.08 ± 0.08	0.28 ± 0.09	0.07
11			Main effect of time		F(3,143)= 1.15	0.329				
12			Interaction, AEA × time		F(3,429)= 0.11	0.043	*			
13	Figure 2F Figure S1C	HB101 OD 0.5 DA837 OD 2.2	Two-factor ANOVA, repeated measures	*n= 96 (AEA–)* *n=35 (AEA+)*						
14			Main effect of AEA		F(1,129)= 5.26	0.023	*	-0.16 ± 0.08	0.01 ± 0.17	0.04
15			Main effect of time		F(3,129)= 0.70	0.448				
16			Interaction, AEA × time		F(3,387)= 0.63	0.402				
17	Figure 2G [(a)]	DA1877 OD 1	Two-factor ANOVA, repeated measures	*n=41 (AEA–)* *n=40 (AEA+)*						
18			Main effect of AEA		F(1,79)= 23.57	0.000	***	0.42 ± 0.03	0.54 ± 0.03	0.22
19			Main effect of time		F(3,79)= 75.42	0.000	***			
20			Interaction, AEA × time		F(3,237)= 3.80	0.011	*			
21	Figure 2G [(a)]	DA1885 OD 1	Two-factor ANOVA, repeated measures	*n=41 (AEA–)* *n=40 (AEA+)*						
22			Main effect of AEA		F(1,79)= 4.74	0.033	*	0.15 ± 0.03	0.11 ± 0.02	0.06
23			Main effect of time		F(3,79)= 32.05	0.0000	***			
24			Interaction, AEA × time		F(3,237)= 1.74	0.1596				

Table S2. Statistics for Figures 2 and S1 A-C.

Preference index over time (line 1-16) or fraction of worms in specified food over time (line 17-24) in T-mazes ± AEA. Unit of replication: assay plate (7-117 animals per plates). Experimental conditions are described in column 3. Stars in the Significance column indicate significance levels: *, $p < 0.05$; **, $p < 0.01$; ***, $p < 0.001$. Effect sizes were computed as described in Materials and Methods and 95% confidence intervals were used as a dispersion measure. (a) Same data as in Figure 2B

Line	Figure	Condition	Test	Number of replicates	Statistic	p-value	Significance	Condition 1 avg +/-CI	Condition 2 avg +/-CI	Effect size
1	Figure 3A	DA1877 OD 0.5 DA1885 OD 3 + sodium azide	Two-factor ANOVA, repeated measures	*n=12 (AEA–)* *n=12 (AEA+)*						
2			Main effect of AEA		F(1,22)= 11.71	0.002	**	0.08 ± 0.09	0.26 ± 0.07	0.35
3			Main effect of time		F(3,22)= 3.70	0.016	*			
4			Interaction, AEA × time		F(3,66)= 0.26	0.146				
5	Figure 3B Figure S2A,B [(a)]	DA1877 OD 0.5 DA1885 OD 8 *ceh-36* vs N2	Two-factor ANOVA	*N2 n=86 (AEA–)* *n=59 (AEA+)* *ceh-36 n=24 (AEA–)* *n=21 (AEA+)*						
6			Main effect of strain		F(1,79)= 3.27	0.074				
7			Main effect of AEA		F(1,79)= 1.98	0.164				
8			Interaction, AEA × strain		F(1,79)= 3.15	0.080				
9			Planned comparisons, t-test							
10			N2, AEA– vs AEA+		t(79)= -2.16	0.034	*	0.34 ± 0.20 (AEA–)	0.58 ± 0.13 (AEA+)	0.67
11			*ceh-36*, AEA– vs AEA+		t(79)= -0.27	0.787		0.34± 0.15 (AEA–)	0.32 ± 0.12 (AEA+)	
12			AEA–, N2 vs ceh-36		t(79)= 0.02	0.981		0.34 ± 0.20 (N2)	0.34± 0.15 (*ceh-36*)	
13			AEA+, N2 vs *ceh-36*		t(79)= 2.53	0.013	*	0.58 ± 0.13 (N2)	0.32 ± 0.12 (*ceh-36*)	-1.0
14	Figure 3D	N2 DA1877 OD 1 vs DA1885 OD 1	Two-factor ANOVA	*DA1877 n= 28 (AEA –)* *n= 32 (AEA+)* *DA1885 n= 30 (AEA –)* *n= 29 (AEA+)*						
15			Main effect of bacteria		F(1,115)= 3.17	0.078				
16			Main effect of AEA		F(1,115)= 0.89	0.349				
17			Interaction, AEA × bacteria		F(1,115)= 11.98	0.001	***			
18			Planned comparisons, t-test							
19			DA1877 AEA– vs AEA+		t(58)= -2.68	0.010	**	1.98 ± 0.62 (AEA–)	3.38 ± 0.83 (AEA+)	0.34
20			DA1885 AEA– vs AEA+		t(57)= -2.23	0.030	*	2.56 ± 0.53 (AEA–)	1.75 ± 0.53 (AEA+)	-0.4
21			AEA– DA1877 vs DA1885		t(56)= 1.45	0.152		1.98 ± 0.62 (DA1877)	2.56 ± 0.53 (DA1885)	
22			AEA+ DA1877 vs DA1885		t(59)= -3.30	0.002	**	3.38 ± 0.83 (DA1877)	1.75 ± 0.53 (DA1885)	0.4

Table S3. Statistics for Figures 3 and S2 A-B.

Line 1-13, Preference index over time in T-maze ± AEA. Unit of replication: assay plate (16-135 animals per plates). Line 14-22 ΔF/F in AWC ± AEA. Unit of replication: individual worm. Experimental conditions are described in column 3. Stars in the Significance column indicate significance levels: *, $p < 0.05$; **, $p < 0.01$; ***, $p < 0.001$. Effect sizes were computed as described in Materials and Methods and 95% confidence intervals were used as a dispersion measure. (a) Same N2 data as in Figure 2E.

Line	Figure	Condition	Test	Number of replicates	Statistic	p-value	Significance	Condition 1 avg +/-CI	Condition 2 avg +/-CI	Effect size
1	Figure 4A Figure S2E, F [(a)]	DA1877 OD 0.5 DA1885 OD 8 *npr-19(ok2068)* vs N2	Two-factor ANOVA	*N2 n=86 (AEA–)* *n=59 (AEA+)* *npr-19(ok2068) n=24 (AEA–)* *n=24 (AEA+)*						
2			Main effect of strain		F(1,189)= 1.29	0.257				
3			Main effect of AEA		F(1,189)= 5.15	0.024	*			
4			Interaction, AEA × strain		F(1,189)= 1.58	0.210				
5			Planned comparisons, t-test							
6			N2, AEA– vs AEA+		t(189)= -3.49	0.001	**	0.08 ± 0.08 (AEA–)	0.28 ± 0.09 (AEA+)	0.56
7			*npr-19* null, AEA– vs AEA+		t(189)= 0.59	0.559		0.08 ± 0.14 (AEA–)	0.14 ± 0.1 (AEA+)	
8			AEA–, N2 vs *npr-19* null		t(189)= -0.09	0.931		0.08 ± 0.08 (N2)	0.08 ± 0.14 (*npr-19(ok2068)*)	
9			AEA+, N2 vs *npr-19* null		t(189)= 1.66	0.100		0.28 ± 0.09 (N2)	0.14 ± 0.1 (*npr-19(ok2068)*)	
5	Figure 4ª Figure S2C,D	DA1877 OD 0.5 DA1885 OD 8 *npr-19(tm2574)* vs N2	Two-factor ANOVA	*N2 n=108 (AEA–)* *n=108 (AEA+)* *npr-19(tm2574) n=108 (AEA–)* *n=106 (AEA+)*						
6			Main effect of strain		F(1,427)= 31.05	0.000	***			
7			Main effect of AEA		F(1,427)= 5.53	0.019	*			
8			Interaction, AEA × strain		F(1,427)=2.32	0.129				
9			Planned comparisons, t-test							
10			N2, AEA– vs AEA+		t(214)= -2.90	0.004	**	0.39 ± 0.05 (AEA–)	0.49 ± 0.05 (AEA+)	0.39
11			*npr-19*, AEA– vs AEA+		t(212)= -0.55	0.582		0.28 ± 0.06 (AEA–)	0.30 ± 0.06 (AEA+)	
12			AEA–, N2 vs *npr-19*		t(214)= 2.86	0.005	**	0.39 ± 0.05 (N2)	0.28 ± 0.06 (*npr-19(tm2574)*)	
13			AEA+, N2 vs *npr-19*		t(212)= 5.01	0.000	***	0.49 ± 0.05 (N2)	0.28 ± 0.06 (*npr-19(tm2574)*)	0.69
14	Figure 4ª Figure S2C, G [(a)]	DA1877 OD 0.5 DA1885 OD 8 *npr-19* rescue vs N2	Two-factor ANOVA	*N2 n=86 (AEA–)* *n=59 (AEA+)* *npr-19 rescue n= 24 (AEA–)* *n= 2 4(AEA+)*						
15			Main effect of strain		F(1,189)= 0.92	0.339				
16			Main effect of AEA		F(1,189)= 14.58	0.000	***			
17			Interaction, AEA × strain		F(1,189)= 0.02	0.879				
18			Planned comparisons, t-test							
19			N2, AEA– vs AEA+		t(189)= -3.63	0.000	***	0.08 ± 0.08 (AEA–)	0.28 ± 0.09 (AEA+)	0.56
20			*npr-19* rescue, AEA– vs AEA+		t(189)= 2.30	0.022	*	0.02 ± 0.09 (AEA–)	0.23 ± 0.09 (AEA+)	1.13
21			AEA–, N2 vs *npr-19* rescue		t(189)= 0.81	0.421		0.08 ± 0.08 (N2)	0.02 ± 0.09 (*npr-19 rescue*)	

22			AEA+, N2 vs *npr-19* rescue		t(189)= 0.56	0.578		0.28 ± 0.09 (N2)	0.23 ± 0.09 (*npr-19 rescue*)	
23	Figure 4[a] Figure S2C, H [(a)]	ßDA1877 OD 0.5 DA1885 OD 8 CNR1 rescue vs N2	Two-factor ANOVA	*N2 n=86 (AEA–) n=59 (AEA+) CB1 rescue n= 27(AEA–) n= 27 (AEA+)*						
24			Main effect of strain		F(1,195)= 0.97	0.325				
25			Main effect of AEA		F(1,195)= 19.88	0.000	***			
26			Interaction, AEA × strain		F(1,195)= 0.41	0.521				
27			Planned comparisons, t-test							
28			N2, AEA– vs AEA+		t(195)= -3.61	0.000	***	0.08 ± 0.08 (AEA–)	0.28 ± 0.09 (AEA+)	0.56
29			CNR1 rescue, AEA– vs AEA+		t(195)= 3.00	0.003	**	0.09 ± 0.1 (AEA–)	0.36 ± 0.09 (AEA+)	1.13
30			AEA–, N2 vs CNR1 rescue		t(195)= -0.25	0.803		0.08 ± 0.08 (N2)	0.09 ± 0.1 (*CNR1 rescue*)	
31			AEA+, N2 vs CNR1 rescue		t(195)= -1.123	0.263		0.28 ± 0.09 (N2)	0.36 ± 0.09 (*CNR1 rescue*)	
32	Figure 4C [(b)]	DA1877 OD 1 *npr-19(ok2068)* vs N2	Two-factor ANOVA	*N2 n= 28 (AEA–) n= 32 (AEA+) npr-19(ok2068) n= 35 (AEA+) n= 35 (AEA+)*						
33			Main effect of strain		F(1,126)= 1.67	0.198				
34			Main effect of AEA		F(1,126)= 1.60	0.208				
35			Interaction strain × AEA		F(1,126)= 5.42	0.022	*			
36			Planned comparisons, t-test							
37			*npr-19* AEA– vs AEA+		t(68)= -0.63	0.532		3.36 ± 0.90 (AEA–)	3.04 ± 0.47 (AEA+)	
38			N2 AEA– vs AEA+		t(58)= -2.67627	0.010	**	1.98 ± 0.62 (AEA–)	3.38 ± 0.83 (AEA+)	0.34
39			AEA– N2 vs *npr-19*		t(61)= 2.51	0.015	*	1.98 ± 0.62 (N2)	3.36 ± 0.90 (*npr-19*)	0.26
40			AEA+ N2 vs *npr-19*		t(65)= -0.71	0.480		3.38 ± 0.83 (N2)	3.04 ± 0.47 (*npr-19*)	
41	Figure 4C [(b)]	DA1885 OD 1 *npr-19(ok2068)* vs N2	Two-factor ANOVA	*N2 n= 30 (AEA–) n= 29 (AEA+) npr-19(ok2068) n= 37 (AEA+) n= 36 (AEA+)*						
42			Main effect of strain		F(1,128)= 50.22	0.000	***			
43			Main effect of AEA		F(1,128)= 3.79	0.054				
44			Interaction strain × AEA		F(1,128)= 0.13	0.721				
45			Planned comparisons, t-test							
46			*npr-19* AEA– vs AEA+		t(71)= -1.02	0.310		4.90 ± 0.87 (AEA-)	4.33 ± 0.63 (AEA+)	
47			N2 AEA– vs AEA+		t(57)= -2.23	0.030	*	2.56 ± 0.53 (AEA–)	1.75 ± 0.53 (AEA+)	-0.42
48			AEA– N2 vs *npr-19*		t(65)= 4.55	0.000	***	2.56 ± 0.53 (N2)	4.90 ± 0.87 (*npr-19*)	0.47
49			AEA+ N2 vs *npr-19*		t(63)= 6.31	0.000	***	1.75 ± 0.53 (N2)	4.33 ± 0.63 (*npr-19*)	0.89

Table S4. Statistics for Figures 4 and S2 C-H.

Line 1-31 Preference index over time in T-maze ± AEA. Unit of replication: assay plate (4-150 animals per plates). Line 32-49 ΔF/F in AWC ± AEA. Unit of replication: individual worm. Experimental conditions and comparisons tested are described in column 3. Stars in the Significance column indicate significance levels: *, $p < 0.05$; **, $p < 0.01$; ***, $p < 0.001$. Effect sizes were computed as described in Materials and Methods and 95% confidence intervals were used as a dispersion measure. (a) Same N2 data as in Figure 2E, (b) Same N2 data as in Figure 3D.

Line	Figure	Condition	Test	Number of replicates	Statistic	p-value	Significance	Condition 1 avg ± CI	Condition 2 avg ± CI	Effect size
1	Figure S3B [(a)]	DA1877 OD 1 *npr-19* rescue vs N2	Two-factor ANOVA	*npr-19* rescue n=21 (AEA–) n=14 (AEA+) N2 n=28 (AEA–) n=32 (AEA+)						
2			Main effect of strain		F(1,92)=62.05	0.000	***			
3			Main effect of AEA		F(1,92)=4.69	0.033	*			
4			Interaction, AEA × strain		F(1,92)=2.59	0.111				
5			Planned comparisons, t-test							
6			*npr-19* rescue AEA– vs AEA+		t(30)= -0.11	0.909		6.00 ± 0.84 (AEA–)	6.08 ± 0.89 (AEA+)	
7			N2 AEA– vs AEA+		t(58)= -2.68	0.010	**	1.98 ± 0.62 (AEA–)	3.38 ± 0.83 (AEA+)	0.34
8			AEA– N2 vs *npr-19* rescue		t(38)= -7.52	0.000	***	1.98 ± 0.62 (N2)	6.00 ± 0.84 (*npr-19 rescue*)	2.20
9			AEA+ N2 vs *npr-19* rescue		t(31)= -4.33	0.000	***	3.38 ± 0.8 (N2)	6.08 ± 0.89 (*npr-19 rescue*)	1.25
10	Figure S3B [(a)]	DA1885 OD 1 *npr-19* rescue vs N2	Two-factor ANOVA	*npr-19* rescue n=26 (AEA–) n=26 (AEA+) N2 n=30 (AEA–) n=29 (AEA+)						
11			Main effect of strain		F(1,107)=14.18	0.000	***			
12			Main effect of AEA		F(1,107)=11.80	0.000	***			
13			Interaction, AEA × strain		F(1,107)=0.85	0.358				
14			Planned comparisons, t-test							
15			*npr-19* rescue AEA– vs AEA+		t(46)=2.62	0.012	*	4.04 ± 0.82 (AEA-)	2.65 ± 0.61 (AEA+)	-0.73
16			N2 AEA– vs AEA+		t(57)=-2.23	0.030	*	2.56 ± 0.53 (AEA–)	1.75 ± 0.53 (AEA+)	-0.4
17			AEA– N2 vs *npr-19* rescue		t(42)=-2.99	0.005	**	2.56 ± 0.5 (N2)	4.04 ± 0.82 (*npr-19* rescue)	
18			AEA+ N2 vs *npr-19* rescue		t(49)=2.21	0.03	*	1.75 ± 0.53 (N2)	2.65 ± 0.61 (*npr-19 rescue*)	0.60
19										
20	Figure S3D [(a)]	DA1877 OD 1 CNR1 rescue vs N2	Two-factor ANOVA	CB1 rescue n=22 (AEA–) n=28 (AEA+) N2 n=28 (AEA–) n=32 (AEA+)						
21			Main effect of strain		F(1,106)=0.23	0.629				

22			Main effect of AEA		F(1,106)=14.84	0.000	**			
23			Interaction, AEA × strain		F(1,106)=0.11	0.740				
24			Planned comparisons, t-test							
25			CNR1 rescue AEA– vs AEA+		t(48)=3	0.005	**	1.99 ± 0.51 (AEA–)	3.64 ± 0.96 (AEA+)	-0.38
26			N2 AEA– vs AEA+		t(58)=-2.68	0.010	**	1.98 ± 0.62 (AEA–)	3.38 ± 0.83 (AEA+)	0.34
27			AEA– N2 vs CNR1 rescue		t(48)=0.02	0.988		1.98 ± 0.62 (N2)	1.99 ± 0.51 (CNR1 *rescue*)	
28			AEA+ N2 vs CB1 rescue		t(58)=0.42	0.674		3.38 ± 0.8 (N2)	3.64 ± 0.96 (CNR1 *rescue*)	
29	Figure S3D [(a)]	DA1885 OD 1 CNR1 rescue vs N2	Two-factor ANOVA	CB1 rescue n=26 (AEA–) n=24 (AEA+) N2 n=30 (AEA–) n=29 (AEA+)						
30			Main effect of strain		F(1,105)=0.03	0.859				
31			Main effect of AEA		F(1,105)=0.22	0.638				
32			Interaction, AEA × strain		F(1,105)=14.74	0.011	*			
33			Planned comparisons, t-test							
34			CB1 rescue AEA– vs AEA+		t(48)=1.48	0.146		1.89 ± 0.5 (AEA-)	2.55 ± 0.74 (AEA+)	
35			N2 AEA– vs AEA+		t(57)=-2.23	0.030	*	2.56 ± 0.53 (AEA–)	1.75 ± 0.53 (AEA+)	-0.4
36			AEA– N2 vs CNR1 rescue		t(54)=-1.89	0.064		2.56 ± 0.5 (N2)	1.89 ± 0.47 (CNR1 *rescue*)	
37			AEA+ N2 vs CNR1 rescue		t(51)=1.76	0.085		1.75 ± 0.5 (N2)	2.55 ± 0.74 (CNR1 *rescue*)	

Table S5. Statistics for Figure S3B, D, Related to Figure 4.

ΔF/F in AWC ± AEA. Unit of replication: individual worm. Experimental conditions and comparisons tested are described in column 3. Stars in the Significance column indicate significance levels: *, $p < 0.05$; **, $p < 0.01$; ***, $p < 0.001$. Effect sizes were computed as described in Materials and Methods and 95% confidence intervals were used as a dispersion measure. (a) Same N2 data as in Figure 3D.

		Number of GFP positive cells			
		Head			Tail
Worm #	1	28	Worm #	1	7
	2	22		2	9
	3	33		3	10
	4	30		4	9
	5	28		5	9
	6	33		6	8
	7	28		7	9
	8	29		8	8
	9	36		9	7
	10	26		10	9
	11	19		11	8
	12	26		12	7
	13	36		13	9
	14	35		14	8
	15	34		15	7
	16	29		16	9
	17	32		17	8
	18	26		18	7
	19	26		19	8
	20	27		20	7
	21			21	10
	22			22	8
Mean ± 95% CI		29.2 ± 2.1	Mean ± 95% CI		8.2 ± 0.4

Table S6. Counts of npr-19-expressing neurons in the head and tail, Related to Figure 5.

Number of p*npr-19*::GFP positive neurons present in the head (n = 20 worms), or the tail (n = 22 worms).

Line	Figure	Condition	Test	Number of replicates	Statistic	p-value	Significance	Condition 1 avg +/-CI	Condition 2 avg +/-CI	Effect size
1	5C	DA1877 OD 1 *unc-13* vs N2	Two-factor ANOVA	*unc-13 n= 27 (AEA–)* *n= 27 (AEA+)* *N2 n= 28 (, AEA–)* *n= 32 (AEA+)*						
2			Main effect of strain		F(1,109)= 6.650	0.011	*			
3			Main effect of AEA		F(1,109)= 17.031	0.000	***			
4			Interaction, AEA × strain		F(1,109)= 0.134					
5			Planned comparisons, t-test							
6			*unc-13* AEA– vs AEA+		t(51)= 3.22	0.002	**	2.83 ± 0.66 (AEA–)	4.49 ± 0.77 (AEA+)	0.47
7			N2 AEA– vs AEA+		t(58)= -2.68	0.010	**	1.98 ± 0.62 (AEA–)	3.38 ± 0.83 (AEA+)	0.34
8			AEA– N2 vs *unc-13*		t(52)= 1.87	0.067		1.98 ± 0.6 (N2)	2.83 ± 0.66 (*unc-13*)	
9			AEA+ N2 vs *unc-13*		t(57)= 1.97	0.054		3.38 ± 0.8 (N2)	4.49 ± 0.77 (*unc-13*)	
10	5C	DA1885 OD 1 *unc-13* vs N2	Two-factor ANOVA	*unc-13 n= 32 (AEA–)* *n= 33 (AEA+)* *N2 n= 30 (AEA–)* *n= 29 (AEA+)*						
11			Main effect of strain		F(1,120)= 3.94	0.050	*			
12			Main effect of AEA		F(1,120)= 10.80	0.001	**			
13			Interaction, AEA × strain		F(1,120)= 0.20	0.658				
14			Planned comparisons, t-test							
15			*unc-13* AEA– vs AEA+		t(63)= -2.42	0.019	*	2.56 ± 0.5 (AEA-)	2.2 ± 0.47 (AEA+)	-0.34
16			N2 AEA– vs AEA+		t(57)= -2.23	0.030	*	2.56 ± 0.53 (AEA–)	1.75 ± 0.53 (AEA+)	-0.4
17			AEA– N2 vs *unc-13*		t(60)= 1.58	0.119		2.56 ± 0.5 (N2)	3.27 ± 0.72 (*unc-13*)	
18			AEA+ N2 vs *unc-13*		t(60)= 1.31	0.197		1.75 ± 0.5 (N2)	2.2 ± 0.47 (*unc-13*)	
19	5E	DA1877 OD 1 *unc-31* vs N2	Two-factor ANOVA	*unc-31 n= 25 (AEA–)* *n= 24 (AEA+)* *N2 n= 28 (AEA–)* *n= 32 (AEA+)*						
20			Main effect of strain		F(1,99)-=1.98	0.163				
21			Main effect of AEA		F(1,99)=1.22	0.271				
22			Interaction, AEA × strain		F(1,99)=9.54	0.003	**			
23			Planned comparisons, t-test							
24			*unc-31* AEA– vs AEA+		t(47)= -1.75	0.087		2.62 ± 0.73 (AEA–)	1.8 ± 0.57 (AEA+)	
25			N2 AEA– vs AEA+		t(58)= -2.68	0.010	**	1.98 ± 0.62 (AEA–)	3.38 ± 0.83 (AEA+)	0.34
26			AEA– N2 vs *unc-31*		t(51)= 1.34	0.187		1.98 ± 0.6 (N2)	2.62 ± 0.73 (*unc-31*)	
27			AEA+ N2 vs *unc-31*		t(54)= -3.15	0.003	**	3.38 ± 0.8 (N2)	1.8 ± 0.57 (*unc-31*)	-0.40

28	5E	DA1885 OD 1 *unc-31* vs N2	Two-factor ANOVA	*unc-31* n= 19 (AEA–) n= 25 (AEA+) N2 n= 30 (AEA–) n= 29 (AEA+)						
29			Main effect of strain		F(1,99)= 0.13	0.717				
30			Main effect of AEA		F(1,99)= 3.78	0.055				
31			Interaction, AEA × strain		F(1,99)= 11.26	0.001	**			
32			Planned comparisons, t-test							
33			*unc-31* AEA– vs AEA+		t(42)= 2.42	0.020	*	2.56 ± 0.5 (AEA-)	3.31 ± 0.68 (AEA+)	0.43
34			N2 AEA– vs AEA+		t(57)= -2.23	0.030	*	2.56 ± 0.53 (AEA–)	1.75 ± 0.53 (AEA+)	-0.4
35			AEA– N2 vs *unc-31*		t(47)= -1.1	0.281		2.56 ± 0.5 (N2)	2.04 ± 0.76 (*unc-31*)	
36			AEA+ N2 vs *unc-31*		t(52)= 3.61	0.001	***	1.75 ± 0.5 (N2)	3.31 ± 0.68 (*unc-31*)	0.64

Table S7. Statistics for Figure 5.

ΔF/F in AWC ± AEA. Unit of replication: individual worm. Experimental conditions and comparisons tested are described in column 3. Stars in the Significance column indicate significance levels: *, $p < 0.05$; **, $p < 0.01$; ***, $p < 0.001$. Effect sizes were computed as described in Materials and Methods and 95% confidence intervals were used as a dispersion measure.